539206

PCT/GB 2003 / 005673

PATENTS • DESIGNS • COPYRIGHT • TRADE MARKS

The Patent Office

INVESTOR IN PEOPLE

The Patent Office
Concept House
Cardiff Road
Newport
South Wales
NP10 8QQ

RECEIVED
03 FEB 2004
WIPO PCT

I, the undersigned, being an officer duly authorised in accordance with Section 74(1) and (4) of the Deregulation & Contracting Out Act 1994, to sign and issue certificates on behalf of the Comptroller-General, hereby certify that annexed hereto is a true copy of the documents as originally filed in connection with the patent application identified therein.

In accordance with the Patents (Companies Re-registration) Rules 1982, if a company named in this certificate and any accompanying documents has re-registered under the Companies Act 1980 with the same name as that with which it was registered immediately before re-registration save for the substitution as, or inclusion as, the last part of the name of the words "public limited company" or their equivalents in Welsh, references to the name of the company in this certificate and any accompanying documents shall be treated as references to the name with which it is so re-registered.

In accordance with the rules, the words "public limited company" may be replaced by p.l.c., plc, P.L.C. or PLC.

Re-registration under the Companies Act does not constitute a new legal entity but merely subjects the company to certain additional company law rules.

Signed

Dated 20 January 2004

PRIORITY DOCUMENT

SUBMITTED OR TRANSMITTED IN COMPLIANCE WITH RULE 17.1(a) OR (b)

Patents Form 1/77

Patents Act 1977
(Rule 16)

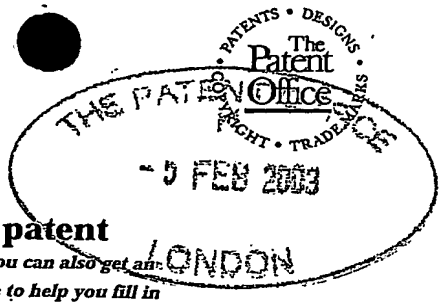

1/77

Request for grant of a patent

(See the notes on the back of this form. You can also get an explanatory leaflet from the Patent Office to help you fill in this form)

The Patent Office

Cardiff Road
Newport
South Wales
NP10 8QQ

1. Your reference 9315 GB MPC/EAD

06FEB03 E782667-1 D00001
P01/7700 0.00-0302632.5

2. Patent application number
(The Patent Office will fill in this part) 05 FEB 2003 0302632.5

3. Full name, address and postcode of the or of each applicant *(underline all surnames)*

BlazePhotonics Limited
Finance Office
University of Bath
The Avenue
Claverton Down
Bath BA2 7AY

Patents ADP number *(if you know it)* 08141129001

If the applicant is a corporate body, give the country/state of its incorporation: United Kingdom

4. Title of the invention: Enhanced Optical Waveguide

5. Name of your agent *(if you have one)*: Abel & Imray

"Address for service" in the United Kingdom to which all correspondence should be sent *(including the postcode)*:

20 Red Lion Street
London
WC1R 4PQ
United Kingdom

Patents ADP number *(if you know it)*: 174001 ✓

6. If you are declaring priority from one or more earlier patent applications, give the country and the date of filing of the or of each of these earlier applications and *(if you know it)* the or each application number

Country	Priority application number *(if you know it)*	Date of filing *(day / month / year)*

7. If this application is divided or otherwise derived from an earlier UK application, give the number and the filing date of the earlier application

Number of earlier application	Date of filing *(day / month / year)*

8. Is a statement of inventorship and of right to grant of a patent required in support of this request? *(Answer 'Yes' if:*

a) any applicant named in part 3 is not an inventor, or
b) there is an inventor who is not named as an applicant, or
c) any named applicant is a corporate body.
See note (d))

Yes

Patents Form 1/77

9. Enter the number of sheets for any of the following items you are filing with this form. Do not count copies of the same document

Continuation sheets of this form	
Description	30
Claim(s)	9
Abstract	
Drawing(s)	15 x15

10. If you are also filing any of the following, state how many against each item.

Priority documents	
Translations of priority documents	
Statement of inventorship and right to grant of a patent *(Patents Form 7/77)*	
Request for preliminary examination and search *(Patents Form 9/77)*	1
Request for substantive examination *(Patents Form 10/77)*	
Any other documents *(please specify)*	

11. I/We request the grant of a patent on the basis of this application.

Signature Abel & Imray Date 05/02/03

12. Name and daytime telephone number of person to contact in the United Kingdom: Matthew Critten - 01225 469 914

Warning

After an application for a patent has been filed, the Comptroller of the Patent Office will consider whether publication or communication of the invention should be prohibited or restricted under Section 22 of the Patents Act 1977. You will be informed if it is necessary to prohibit or restrict your invention in this way. Furthermore, if you live in the United Kingdom, Section 23 of the Patents Act 1977 stops you from applying for a patent abroad without first getting written permission from the Patent Office unless an application has been filed at least 6 weeks beforehand in the United Kingdom for a patent for the same invention and either no direction prohibiting publication or communication has been given, or any such direction has been revoked.

Notes

a) *If you need help to fill in this form or you have any questions, please contact the Patent Office on 08459 500505.*

b) *Write your answers in capital letters using black ink or you may type them.*

c) *If there is not enough space for all the relevant details on any part of this form, please continue on a separate sheet of paper and write "see continuation sheet" in the relevant part(s). Any continuation sheet should be attached to this form.*

d) *If you have answered 'Yes' Patents Form 7/77 will need to be filed.*

e) *Once you have filled in the form you must remember to sign and date it.*

f) *For details of the fee and ways to pay please contact the Patent Office.*

Enhanced Optical Waveguide

(Ref: 0066)

Technical Field

The present invention is in the field of optical waveguides and relates in particular to optical waveguides that guide light by virtue of a photonic bandgap.

Background Art

Optical fibre waveguides, which are able to guide light by virtue of a so-called photonic bandgap (PBG), were first proposed in 1995.

In, for example, "Full 2-D photonic bandgaps in silica/air structures", Birks et al., Electronics Letters, 26 October 1995, Vol. 31, No. 22, pp.1941-1942, it was proposed that a PBG may be created in an optical fibre by providing a dielectric cladding structure, which has a refractive index that varies periodically between high and low index regions, and a core defect in the cladding structure in the form of a hollow core. In the proposed cladding structure, periodicity was provided by an array of air holes that extended through a silica glass matrix material to provide a PBG structure through which certain wavelengths of light could not pass. It was proposed that light coupled into the hollow core defect would be unable to escape into the cladding due to the PBG and, thus, the light would remain localised in the core defect.

It was appreciated that light travelling through a hollow core defect, for example filled with air or even under vacuum, would suffer significantly less from undesirable effects, such as non-linearity and loss, compared with light travelling through a solid silica or doped silica fibre core. As such, it was appreciated that a PBG fibre may find application as a transmission fibre to transmit light over extremely long distances, for example across the Atlantic Ocean, without undergoing signal regeneration or as a high optical power delivery waveguide. In contrast, for standard index-guiding, single mode optical fibre, signal regeneration is typically required approximately every 80 kilometres.

The first PBG fibres that were attempted by the inventors had a periodic cladding structure formed by a triangular lattice of circular air holes embedded in a solid silica matrix and surrounding a central air core defect. Such fibres were formed by stacking circular or hexagonal capillary tubes, incorporating a core defect into the cladding by omitting a central capillary of the stack, and then heating and drawing the stack, in a one or two step process, to

form a fibre having the required structure. The first fibres made by this process had a core defect formed by the omission of a single capillary from the centre of the cladding structure.

International patent application PCT/GB00/01249 (The Secretary of State for Defence, UK), filed on 21 March 2000, proposed the first PBG fibre to have a so-called seven-cell core defect, surrounded by a cladding comprising a triangular lattice of air holes embedded in an all-silica matrix. The core defect was formed by omitting an inner capillary and, in addition, the six capillaries surrounding the inner capillary. This fibre structure was seen to guide one or two modes in the core defect, in contrast to the previous, single-cell core defect fibre, which appeared not to support any guided modes in the core defect.

According to PCT/GB00/01249, it appeared that the single-cell core defect fibre, by analogy to the density-of-states calculations in solid-state physics, would only support approximately 0.23 modes. That is, it was not surprising that the single-cell core defect fibre appeared to support no guided modes in its core defect. In contrast, based on the seven-fold increase in core defect area (increasing the core defect radius by a factor of $\sqrt{7}$), the seven-cell core defect fibre was predicted to support approximately 1.61 spatial modes in the core defect. This prediction was consistent with the finding that the seven-cell core defect fibre did indeed appear to support at least one guided mode in its core defect.

A preferred fibre in PCT/GB00/01249 was described as having a core defect diameter of around 15μm and an air-filling fraction (AFF) – that is, the proportion by volume of air in the cladding - of greater than 15% and, preferably, greater than 30%.

In "Analysis of air-guiding photonic bandgap fibres", Optics Letters, Vol. 25, No. 2, January 15, 2000, Broeng et al. provided a theoretical analysis of PBG fibres. For a fibre with a seven-cell core defect and a cladding comprising a triangular lattice of near-circular holes, providing an AFF of around 70%, the structure was shown to support one or two air guided modes in the core defect. This was in line with the finding in PCT/GB00/01249.

In the chapter entitled "Photonic Crystal Fibers: Effective Index and Band-Gap Guidance" from the book "Photonic Crystal and Light Localization in the 21st Century", C.M. Soukoulis (ed.), ©2001 Kluwer Academic Publishers, the authors presented further analysis of PBG fibres based primarily on a seven-cell core defect fibre. The optical fibre was fabricated by stacking and drawing hexagonal silica capillary tubes. The authors suggested that a core defect must be large enough to support at least one guided mode but that, as in conventional fibres, increasing the core defect size would lead to the appearance of higher order modes. The authors also went on to suggest that there are many parameters that can

have a considerable influence on the performance of bandgap fibres: choice of cladding lattice, lattice spacing, index filling fraction, choice of materials, size and shape of core defect, and structural uniformity (both in-plane and along the axis of propagation).

WO 02/075392 (Corning, Inc.) identifies a general relationship in PBG fibres between the number of so–called surface modes that exist at the boundary between the cladding and core defect of a PBG fibre and the ratio of the radial size of the core defect and a pitch of the cladding structure, where pitch is the centre to centre spacing of nearest neighbour holes in the triangular lattice of the exemplified cladding structure. It is suggested that when the core defect boundary, together with the photonic bandgap crystal pitch, are such that surface modes are excited or supported, a large fraction of the "light power" propagated along the fibre is essentially not located in the core defect. Accordingly, while surface states exist, the suggestion was that the distribution of light power is not effective to realise the benefits associated with the low refractive index core defect of a PBG crystal optical waveguide. The mode energy fraction in the core defect of the PBG fibre was shown to vary with increasing ratio of core defect size to pitch. In other words, it was suggested that the way to increase mode energy fraction in the core defect is by decreasing the number of surface modes, in turn, by selecting an appropriate ratio of the radial size of the core defect and a pitch of the cladding structure. In particular, WO 02/075392 states that, for a circular core structure, a ratio of core radius to pitch of around 1.07 to 1.08 provides a high mode power fraction of not less than 0.9 and is single mode. Other structures are considered, for example in Figure 7, wherein the core defect covers an area equivalent to 16 cladding holes.

In a Post-deadline paper presented at ECOC 2002, "Low Loss (13dB) Air core defect Photonic Bandgap Fibre", N. Venkataraman et al. reported a PBG fibre having a seven-cell core defect that exhibited loss as low as 13dB/km at 1500nm over a fibre length of one hundred metres. The structure of this fibre closely matches the structure considered in the book chapter referenced above. The authors attribute the relatively small loss of the fibre as being due to the high degree of structural uniformity along the length of the fibre.

PBG fibre structures are typically fabricated by first forming a pre-form and then heating and drawing an optical fibre from that pre-form in a fibre-drawing tower. It is known either to form a pre-form by stacking capillaries and fusing the capillaries into the appropriate configuration of pre-form, or to use extrusion.

For example, in PCT/GB00/01249, identified above, a seven-cell core defect pre-form structure was formed by omitting from a stack of capillaries an inner capillary and, in

addition, the six capillaries surrounding the inner capillary. The capillaries around the core defect boundary in the stack were supported during formation of the pre-form by inserting truncated capillaries, which did not meet in the middle of the stack, at both ends of the capillary stack. The stack was then heated in order to fuse the capillaries together into a pre-form suitable for drawing into an optical fibre. Clearly, only the fibre drawn from the central portion of the stack, with the missing inner seven capillaries, was suitable for use as a hollow core defect fibre.

US patent application number US 6,444,133 (Corning, Inc.), describes a technique of forming a PBG fibre pre-form comprising a stack of hexagonal capillaries in which the inner capillary is missing, thus forming a core defect of the eventual PBG fibre structure that has flat inner surfaces. In contrast, the holes in the capillaries are round. US 6,444,133 proposes that, by etching the entire pre-form, the flat surfaces of the core defect dissolve away more quickly than the curved surfaces of the outer capillaries. The effect of etching is that the edges of the capillaries that are next to the void fully dissolve, while the remaining capillaries simply experience an increase in hole-diameter. Overall, the resulting pre-form has a greater fraction of air in the cladding structure and a core defect that is closer to a seven-cell core defect than a single cell core defect.

PCT patent application number WO 02/084347 (Corning, Inc.) describes a method of making a pre-form comprising a stack of hexagonal capillaries of which the inner capillaries are preferentially etched by exposure to an etching agent. Each capillary has a hexagonal outer boundary and a circular inner boundary, as illustrated in the diagram in Figure 10 herein. The result of the etching step is that the centres of the edges of the hexagonal capillaries around the central region dissolve more quickly than the corners, thereby causing formation of a core defect. In some embodiments, the circular holes are offset in the inner hexagonal capillaries of the stack so that each capillary has a wall that is thinner than its opposite wall. These capillaries are arranged in the stack so that their thinner walls point towards the centre of the structure. An etching step, in effect, preferentially etches the thinner walls first, thereby forming a seven-cell core defect.

Disclosure of the Invention

In arriving at the present invention, the inventors have demonstrated that, while the size of a core defect are significant in determining certain characteristics of a PBG waveguide, the form of a boundary at the interface between core and cladding also plays a significant role

in determining certain characteristics of the waveguide. As will be described in detail hereafter, the inventors have determined that, for given PBG core and cladding structures, variations in only the form of the boundary can cause significant changes in the characteristics of a respective waveguide.

According to a first aspect, the present invention provides an optical waveguide, having a plane cross section and a length dimension, which extends perpendicular to the plane cross section, comprising:

a photonic bandgap structure for providing a photonic bandgap over a range of frequencies of light, the photonic bandgap structure comprising, in the plane cross section, an arrangement of relatively low refractive index regions interspersed with relatively high refractive index regions, which extend parallel to the length dimension;

a core defect comprising a region of relatively low refractive index, which extends parallel to the length dimension and through the photonic bandgap structure; and

a boundary at the interface between the core defect and the photonic bandgap structure, the boundary, in the plane cross section, comprising a plurality of relatively high refractive index boundary veins joined end-to-end around the boundary between boundary nodes, each boundary vein having a length l and a thickness t, at the mid-point along the length l, and being joined between a leading boundary node and a following boundary node, and each boundary node having a diameter and being joined between two boundary veins and to a relatively high refractive index region of the photonic bandgap structure, wherein, in the plane cross section, around the boundary:

$t < d_L$ and $t < d_F$ is true for more than half of the boundary veins; and

$l \geq x(d_L+d_F)$ is true for at least one boundary vein,

where $x \geq 0.6$ and d_L, d_F are the diameters of the leading and following nodes respectively for each vein.

The diameter of a node may be measured as the diameter of the largest circle that fits within the region that makes up the node. The length of a vein may be measured along the centre-line of the vein between said largest circles that fit within the nodes at either end of the vein.

Length $l \geq x(d_L+d_F)$ may be true for a plurality of the boundary veins, at least half of the boundary veins or, even, for all of the boundary veins.

The waveguide may be arranged so that $x \geq 0.8$. The waveguide may be arranged so that $x \geq 1.0$. In some embodiments, the waveguide may be arranged so that $x \geq 1.5$, 2.0, 2.5 or even 3.0.

In the plane cross section, the thinnest point along at least some of the boundary veins may be substantially at the mid-point. For example, a vein may be relatively thick at one end, taper down towards a minimum thickness at the mid-point and then thicken back up towards the other end. In some embodiments, each boundary vein has a thinnest point substantially at the midpoint. Alternatively, at least some veins may have a relatively thicker portion at or near the mid-point. For example, a vein may be relatively thick at one end, taper down and thicken back up to a local maximum thickness at the mid-point, which is less than the thickness at the first-mentioned end, and then taper down and thicken back up again towards the other end.

The photonic bandgap structure may comprise an array of relatively low refractive index regions being separated from one another by relatively high refractive index regions. In some embodiments, the array is substantially periodic. However, in principle, the array need not be periodic – see, for example, "Antiresonant reflecting photonic crystal optical waveguides", by N. M. Litchinitser et al., Optics Letters, Volume 27, No. 18, September 15, 2002, pp1592-1594. Although this paper does not provide calculations explicitly for PBG fibres, it does illustrate that photonic bandgaps may be obtained without periodicity.

The array may have a characteristic primitive unit cell and a pitch Λ.

The array may be a substantially triangular array. Other arrays, of course, may be used, for example, square, hexagonal or Kagomé, to name just three.

Given an array with a pitch Λ, it would be possible to relate the thickness of the boundary veins to a pitch of the photonic bandgap structure. For example, the thickness at the midpoint of a plurality of the boundary veins, or in some embodiments substantially all of the boundary veins, may be less than 0.1Λ. In some embodiments, the thickness at the mid-point of a plurality of the boundary veins, or in some embodiments substantially all of the boundary veins, is less than 0.049Λ.

It is highly unlikely in practice that a photonic bandgap structure according to the present invention will comprise a 'perfectly' periodic array, due to imperfections being introduced into the structure during its manufacture and/or perturbations being introduced into the array by virtue of the presence of the core defect. The present invention is intended to

encompass both perfect and imperfect structures. Likewise, any reference to "periodic", "lattice", or the like herein, imports the likelihood of imperfection.

In some embodiments of the present invention, the relatively low refractive index regions in the photonic bandgap structure are separated from one another by relatively high refractive index veins that are joined at nodes, each node having a diameter and each vein having a length and a thickness at the mid-point along the length and being joined at each end to a node.

At least some boundary nodes may have diameters that are significantly smaller than at least some nodes in the photonic bandgap structure. In some embodiments, substantially all boundary nodes have diameters that are significantly smaller than at least some nodes, or even a significant proportion of all nodes, in the photonic bandgap structure.

The diameters of at least some of the nodes within the photonic bandgap structure, or even a significant proportion of all nodes within the photonic bandgap structure, may be significantly larger than the mid-point thickness of the veins that are joined to the respective nodes.

Said nodes in the photonic bandgap structure, which have a significantly larger diameter than the mid-point thickness of the veins that are joined to the nodes, may have a diameter which is at least 1.5 times the thickness of the veins. Indeed, said nodes in the photonic bandgap structure, having a significantly larger diameter than the thickness of the veins that are joined to the nodes, may have a diameter which is at least twice the thickness of the veins.

At least some of the relatively low refractive index regions may be voids filled with air or under vacuum. Alternatively, or in addition, at least some of the relatively low refractive index regions may be voids filled with a gas other than air, for example nitrogen, or a liquid. The region of relatively low refractive index that makes up the core may comprise the same or a different material compared with the regions of relatively low refractive index in the photonic bandgap structure.

In some embodiments, at least some of the relatively high refractive index regions comprise silica glass. The glass may be un-doped or doped with index raising or lowering dopants. Alternatively, the relatively high refractive index may comprise another solid material, for example a different kind of glass or a polymer.

In preferred embodiments, the proportion by volume of relatively low refractive index regions in the photonic bandgap structure is higher than 75%. The proportion by volume may be higher than 80% or even more than 85%, for example around 87.5% or up to 90%.

In preferred embodiments, the waveguide supports a mode having more than 90% of the mode power in relatively low refractive index regions. More preferably, more than 95%, 98% or 99% of the mode power, or even more than 99.5% of the mode power, is in the relatively low refractive index regions.

The waveguide may support a mode having a mode profile that closely resembles the fundamental mode of a standard optical fibre. An advantage of this is that the mode may readily couple into standard, single mode optical fibre.

Alternatively, or in addition, the waveguide may support a non-degenerate mode. This mode may resemble a TE_{01} mode in standard optical fibres.

Preferably, in either case, said mode supports a maximum amount of the mode power in relatively low refractive index regions compared with other modes that are supported by the waveguide.

At least some of the boundary veins may be substantially straight. In some embodiments, substantially all of the boundary veins are substantially straight. Alternatively, or additionally, at least some of the boundary veins may be bowed outwardly from the core defect.

According to a second aspect, the present invention provides an optical fibre comprising a waveguide as described above.

According to a third aspect, the present invention provides a transmission line for carrying data between a transmitter and a receiver, the transmission line including along at least part of its length a fibre as described above.

According to a fourth aspect, the present invention provides a method of forming a photonic bandgap optical waveguide having a plane cross section and a length dimension, which extends perpendicular to the plane cross section, comprising the steps:

forming a preform stack by stacking a plurality of elongate elements;

omitting, or substantially removing at least one elongate element from an inner region of the stack; and

heating and drawing the stack, in one or more steps, into a photonic bandgap optical waveguide,

characterised by a photonic bandgap structure, a core defect and a boundary at the interface between the core defect and the photonic bandgap structure,

the photonic bandgap structure for providing a photonic bandgap over a range of frequencies of light, the photonic bandgap structure comprising, in the plane cross section, an arrangement of relatively low refractive index regions interspersed with relatively high refractive index regions, which extend parallel to the length dimension,

the core defect comprising a region of relatively low refractive index, which extends parallel to the length dimension and through the photonic bandgap structure,

the boundary at the interface between the core defect and the photonic bandgap structure, the boundary, in the plane cross section, comprising a plurality of relatively high refractive index boundary veins joined end-to-end around the boundary between boundary nodes, each boundary vein having a length l and a thickness t, at the mid-point along the length l, and being joined between a leading boundary node and a following boundary node, and each boundary node having a diameter and being joined between two boundary veins and to a relatively high refractive index region of the photonic bandgap structure, wherein, in the plane cross section, around the boundary:

$t < d_L$ and $t < d_F$ is true for more than half of the boundary veins; and

$l \geq x(d_L+d_F)$ is true for at least one boundary vein,

where $x \geq 2$ and d_L, d_F are the diameters of the leading and following nodes respectively for each vein.

The preform stack may comprise a substantially periodic, triangular array of elongate elements.

The elements may have a generally hexagonal transverse cross section or a generally circular transverse cross section.

For generally circular cross section elements, first elongate interstitial voids are formed between elements.

The method may include the additional step of introducing elongate elements into at least some of the first interstitial voids. At least some of the elongate elements may comprise rods. Additionally, or alternatively, at least some of the elongate elements may comprise capillaries. Use of capillaries provides the option to control more closely the volume of glass that is added to an interstitial void for a given outer diameter of capillary. The elongate elements may be introduced into substantially all of the first interstitial voids.

The method may comprise the additional step of introducing a further elongate element into the inner region to support the elements around the inner region. As such, second interstitial voids may be formed between the elements around the inner region and the further elongate element, and the method may include the step of introducing elongate elements into at least some of the second interstitial voids. Again, at least some of the elongate elements may comprise rods. Additionally, or alternatively, at least some of the elongate elements may comprise capillaries.

A reduced fraction of the rods may be introduced into the second interstitial voids compared with the number of rods that are introduced into a similar configuration of first interstitial voids. For example, no elongate elements are introduced into the second interstitial voids.

At least some of the elongate elements that are introduced into the second interstitial voids may have a smaller cross sectional area than the elongate elements that are introduced into the first interstitial voids.

In some embodiments of the present invention, the further elongate element has a relatively low refractive index elongate inner region enclosed by a relatively high refractive index outer region, which becomes part of the photonic bandgap optical waveguide.

Alternatively, the further elongate element comprises a material that has a higher coefficient of thermal expansion than the relatively high refractive index material in the elongate elements. Accordingly, the method may comprise the further steps of:

heating the pre-form stack in order to fuse the elongate elements around the further elongate element;

cooling the pre-form stack; and

removing the further elongate element from the pre-form stack prior to heating and drawing the pre-form stack.

At least some of the relatively low refractive index regions may comprise air or be under vacuum. Alternatively, or in addition, at least some of the relatively low refractive index regions are voids filled with a gas other than air or a liquid.

At least some of the relatively high refractive index regions may comprise silica glass.

Other aspects and embodiments will become apparent from reading the following description and claims and considering the following drawings.

Brief Description of the Drawings

Embodiments of the present invention will now be described, by way of example only, with reference to the accompanying drawings, of which:

Figure 1 is a diagram of a transverse cross section of a PBG fibre structure of the kind known from the prior art;

Figure 2 is a diagram which illustrates how various physical characteristics of PBG fibres are defined herein;

Figures 3 and 4 provide diagrams of various examples of PBG fibre structures;

Figures 5 and 6 provide mode spectra plots for the PBG fibre structures of Figures 3 and 4;

Figure 7 provides mode intensity distribution plots for a mode, supported by each structure of Figures 3 and 4, which supports the highest amount of light in air;

Figures 8 and 9 provide graphs of mode intensity for x and y axes of the distributions of Figure 7;

Figure 10 provides a mode intensity distribution plot for a mode, supported by an alternative structure, which supports the highest amount of light in air;

Figure 11 is a diagram of a pre-form suitable for making PBG fibre according to the prior art;

Figure 12 is a diagram of a pre-form suitable for making a fibre according to embodiments of the present invention;

Figure 13 is a diagram of an alternative pre-form suitable for making a fibre according to embodiments of the present invention; and

Figure 14 is a diagram of a further alternative pre-form suitable for making a fibre according to embodiments of the present invention.

Best Mode For Carrying Out the Invention, & Industrial Applicability

Figure 1 is a representation of a transverse cross-section of a fibre structure of the kind described in the prior art and is used herein as a reference against which the characteristics of other structures described herein are compared. In the Figure, the black regions represent fused silica glass and the white regions represent air holes in the glass. As illustrated, the cladding 100 comprises a triangular array of generally hexagonal cells 105, surrounding a seven-cell core defect 110. A core defect boundary 145 is at the interface between the cladding and the core defect. The core defect boundary has twelve sides – alternating

between six relatively longer sides and six relatively shorter sides - and is formed by omitting or removing seven central cells; an inner cell and the six cells that surround the inner cell. The cells would have typically been removed or omitted from a pre-form prior to drawing the pre-form into the fibre. As the skilled person will appreciate, although a cell comprises a void, or a hole, for example filled with air or under vacuum, the voids or holes may alternatively be filled with a gas or a liquid or may instead comprise a solid material that has a different refractive index than the material that surrounds the hole. Equally, the silica glass may be doped or replaced by a different glass or other suitable material such as a polymer.

Two longitudinal planes through the fibre structure of Figure 1 are denoted y and x; with y being a vertical plane passing through the centre of the structure and x being a horizontal plane passing through the centre of the structure as shown.

Hereafter, and with reference to Figure 1, a region of glass 115 between any two holes is referred to as a "**vein**" and a region of glass 120 where veins meet is referred to as a "**node**".

The core defect boundary 145 comprises the inwardly-facing veins of the innermost ring of cells that surround the core defect 110.

In practice, for triangular lattice structures that have a large air-filling fraction, for example above 75%, most of the cladding holes 105 assume a generally hexagonal form, as shown in Figure 1, and the veins are generally straight.

Figures 2a and 2b are diagrams which illustrate how various dimensions of the cladding structure of Figure 1 are defined herein, with reference to four exemplary cladding cells 200.

For the present purposes, a node 210' in the cladding, which is referred to herein as a "**cladding node**", is said to have a diameter measurement **d** defined by the largest diameter circle that can fit within the glass that forms the node. A vein 205 in the cladding, which is referred to herein as a "**cladding vein**", has a length **l**, measured along its centre-line between the circles of the cladding nodes 210 & 210' to which the cladding vein is joined and a thickness, **t**, measured at its mid-point between the respective cladding nodes. Generally, herein, veins increase in thickness towards the nodes to which they are joined.

The mid-point of a cladding vein is typically the thinnest point along the vein. Unless otherwise stated herein, generally, a specified vein thickness is measured at the mid-point of the vein between the two nodes to which the vein is joined.

According to Figure 2, the periphery of a cladding node is constructed from three notional circular paths 215, each one being positioned between and abutting a different pair of neighbouring cladding veins that join the node. More particularly, the periphery of the node between each pair of veins is defined by the portions of the circular paths 215 which begin at a point p and end at a point q along first and second veins respectively. Points p and q are equidistant from the centre of the node 210'. It will be appreciated that the diameter, d, of the node 210' is a function of the thickness, t, of the veins, the distance of p from the centre of the node and the pitch Λ, or centre to centre distance between neighbouring cells, of the structure.

The cells forming the innermost ring around the boundary of the core defect, which are referred to herein as "**boundary cells**", have one of two general shapes. A first kind of boundary cell 125 is generally hexagonal and has an innermost vein 130 that forms a relatively shorter side of the core defect boundary 145. A second kind of boundary cell 135 has a generally pentagonal form and has an innermost vein 140 that forms a relatively longer side of the core defect boundary 145.

Referring again to Figure 1, there are twelve boundary cells 125, 135 and twelve nodes 150, which are referred to herein as "**boundary nodes**", around the core defect boundary 145. Specifically, as defined herein, there is a boundary node 150 wherever a vein between two neighbouring boundary cells meets the core defect boundary 145. In Figure 1, these boundary nodes 150 have slightly smaller diameters than the cladding nodes 160. Additionally, there is an enlarged region 165, or "**bead**", of silica at the mid point of each relatively longer side of the core defect boundary 145. These beads 165 coincide with the mid-point along the inner-facing vein 140 of each pentagonal boundary cell 135. The beads 165 may result from a possible manufacturing process used to form the structure in Figure 1, as will be described in more detail below. For the present purposes, the veins 130 & 140 that make up the core defect boundary are known as "**boundary veins**".

As will be described below, it is possible to control the diameters of particular nodes and the existence or size of beads along the core defect boundary during manufacture of a fibre.

The structure in Figure 1 and each of the following examples of different structures closely resemble practical optical fibre structures, which have either been made or may be made according to known processes or the processes described hereinafter. The structures share the following common characteristics:

a pitch Λ of the cladding chosen between values of approximately 3μm and 6μm (this value may be chosen to position core-guided modes at an appropriate wavelength for a particular application);

a thickness t of the cladding veins of 0.0586 times the chosen pitch Λ of the cladding structure (or simply 0.0586Λ);

an AFF in the cladding of approximately 87.5%; and

a ratio **R** having a value of about 0.5.

R is defined as the ratio of the distance of p' from the centre of the nearest cladding node to half the length of a cladding vein, **l/2**; where p' is a point along the centre-line of a cladding vein and is defined by a construction line that passes through the centre-line of the vein, the centre of circle 215 and the point p where the circle meets the vein.

In effect, R is a measure of the radius of curvature of the corners of the hexagonal cells within the cladding. It will be apparent that the maximum practical value of R is 1, at which value the radius of curvature is a maximum and the cladding holes are circular. The minimum value of R is dictated by the thickness t and length l of the veins and is the value at which the diameter of the circle 215 tends to zero and the cladding holes are hexagonal.

For all values of R below the maximum value, the veins have a region of generally constant thickness about their mid-points, which increases in length with decreasing R. For example, a value of R=0.5 provides that around half the length of a vein, about its mid-point, has a substantially constant thickness. Likewise, a value of R=0.25 provides that around three quarters of the length of a vein, about its mid-point, has a substantially fixed thickness.

Given R, t and Λ, for practical purposes, the diameter d of the cladding nodes is found to be approximately:

$$d = \frac{2R\Lambda}{\sqrt{3}} - \Lambda R + t \qquad \text{(Equation 1)}$$

In Figure 1, the diameter of each boundary node 150, d_e, is smaller than the diameter of the cladding nodes 160, due to there being less glass available at the boundary for forming the nodes. A model similar to that shown in Figure 2 may if required be used to define the form of the boundary nodes. The differences between Figure 2 and the model for the boundary nodes are (1) the boundary node model includes the core defect 110 and two boundary cells rather than three cladding cells, (2) it is assumed that the value of R is a

minimum, such that there is no measurable circular path inside the core defect 110; and, (3) the internal angles of the core defect and the boundary cells are different from each other and from the cells in the cladding.

The beads 165 shown in Figure 1 are oval shaped, each having a major dimension which is approximately 1/3 the length of the distance between the two node centres that lie on either side of the bead and a minor dimension which is 1/3 the length of the major dimension. The minor dimension of the bead, which defines the thickness of the associated vein at its mid-point, is slightly longer than the diameter of the respective boundary nodes 150.

For boundary veins with no beads, the thickness at the mid-point of the vein between boundary nodes is the same as the thickness of the cladding veins at the same point.

The present inventors have determined that it is possible to control the performance of PBG fibres in particular by aiming to maximise the amount of light that propagates in air within the fibre structure, even if some light is not in the core, in order to benefit from the properties of PBG fibres, such as reduced absorption, non-linearity and, in addition, reduced mode coupling.

For the purposes of comparing aspects of the performance of various different structures it is useful to consider the modes that are supported in the band gap of various PBG fibre structures. This may be achieved by solving Maxwell's vector wave equation for the fibre structures, using known techniques. In brief, Maxwell's equations are recast in wave equation form and solved in a plane wave basis set using a variational scheme. An outline of the method may be found in Chapter 2 of the book "Photonic Crystals – Molding the Flow of Light", J.D. Joannopoulos et al., ©1995 Princeton University Press.

Figures 3 and 4 illustrate six exemplary PBG fibre structures that will be considered hereafter. Figure 3 illustrates three structures identified as S1, S2 and S3 herein, which are seven-cell core defect structures. S1 is the same as the structure illustrated in Figure 1 and is reproduced in Figure 3 for convenience only.

The characteristics of S1 have already been described above. S1 resembles a prior art structure in which the mid-points of the boundary veins with beads have a thickness, due to the beads, that is slightly greater than the diameters of the respective nodes. It is instructive to compare the characteristics of S1 with the other structures herein in order to illustrate how the mode spectra of structures can vary significantly with different boundary characteristics.

Figure 4 illustrates three structures identified as S4, S5 and S6, which have a nineteen-cell core defect. S4, S5 and S6, apart from core defect size, have the same cladding

characteristics as S1, S2 and S3 respectively. S1 to S3 have a maximum core defect radius of 1.5275Λ. In contrast, S4 to S6 have a maximum core defect radius of 2.5166Λ.

The characteristics of structures S2 to S6 will now be described in detail.

There are a number of differences between the form of the boundary in S1 and the boundary in S2. S2 has reduced boundary node diameters, which are significantly smaller than the cladding nodes 360, compared with S1, and no apparent beads along the core defect boundary 345. According to the definitions provided herein, the boundary nodes 355 in S2 have a minimum diameter; the associated values of R are at a minimum and, accordingly, there are no measurable circular paths defining the periphery of the nodes. The diameters of the boundary nodes 355 in S2 are only very slightly larger than the thickness of the boundary veins 330, 340. In contrast, as for S1, the cladding nodes 360 have diameters that are significantly larger than the thickness of their adjoining veins 315.

While S2 is an embodiment of the present invention, it may in practice be difficult to make the exact structure due to surface tension effects acting on the glass during the drawing process, which may cause the cladding veins to meet the boundary veins at slightly rounded corners; meaning R is not its theoretical minimum. However, it is useful to compare the characteristics of S2 with the other structures herein. Structures closely resembling S2, according to embodiments of the present invention, can be made according to a method that will be described in detail below.

The boundary in S3 has no apparent beads, as in S2, and the boundary nodes 355 have a similar diameter to those in S1. S3 represents an exemplary embodiment of the present invention.

The structure in S4 has an additional ring of cladding cells removed from around the core defect compared with S1. This forms a core defect 410 equivalent to nineteen missing cladding cells. Similar to S1, S4 has boundary nodes 450 that are significantly larger in diameter than the thickness of the respective boundary veins and there are hexagonal cells 425 at each corner of the core defect 410. However, in contrast to S1, which has one generally pentagonal cell along each side of the core defect boundary 145, S4 has two generally pentagonal cells 435 along each side of the core defect boundary 445. In addition, there are two beads 455 along each side of the core defect boundary 445, roughly coincident with the mid-point of the vein 440 of each pentagonal cell 425 that borders the core defect boundary 445. The minor dimension of each bead is slightly longer than the diameter of the nodes to which each respective vein is joined. There are also three boundary nodes 455 per relatively

longer side of the core defect boundary 445, compared with two for the seven-cell core defect structures. Overall, S4 has eighteen cells sharing veins with the core defect boundary 445.

The boundary in S5 is similar to S2 in the respect that it has reduced-diameter boundary nodes 455', which do not have diameters that are significantly larger than the thickness of the respective veins, and there are no apparent beads. All other parameters of S5 are the same as S4.

The boundary in S6 has no apparent beads, as in S3, and the boundary nodes 455 have a similar diameter to those in S1. All other parameters of S6 are the same as S4. S6 represents an exemplary embodiment of the present invention.

Figures 5 and 6 each show three mode spectra, identified as P1 to P3 and P4 to P6 respectively. Each spectrum P1 to P6 relates to a respective PBG fibre structure S1 to S6. The horizontal axis of each spectrum is normalised frequency, $\omega\Lambda/c$, where ω is the frequency of the light, Λ is the pitch of the cladding structure, and c is the speed of light in a vacuum. The vertical axis of each spectrum relates to the response of the structure to a given input for a given normalised wave-vector $\beta\Lambda=13$, against which the spectrum is plotted, where β is the chosen propagation constant for the calculations. The spectra are produced using a Finite-difference Time Domain (FDTD) algorithm, which computes the time-dependent response of a given hollow core structure to a given input. This technique has been extensively used in the field of computational electrodynamics, and is described in detail in the book "Computational Electrodynamics: The Finite-Difference Time-Domain Method", A. Taflove & S.C. Hagness, ©2000 Artech House. The FDTD technique may be readily applied to the field of PBG fibres and waveguides by those skilled in the art of optical fibre modelling.

With reference to spectra P1 to P6, each vertical spike indicates the presence of at least one mode at a corresponding normalised frequency. In some cases, multiple modes may appear as a single spike or as a relatively thicker spike compared with other spikes in a spectrum. This is due to the fact that the data used to generate the spectra is not of a high enough resolution to distinguish very closely spaced modes. As such, the mode spectra should be taken to provide only an approximation to the actual numbers of modes that exist for each structure, which is satisfactory for enabling a general comparison between spectra herein.

On each spectrum, a 'light line' for the respective structure is shown as a solid vertical line at $\omega\Lambda/c=13=\beta\Lambda$, and band edges, which bound a bandgap, are represented as two dotted vertical lines, one on either side of the light line, with a lower band edge of the bandgap at

around $\omega\Lambda/c=12.92$ and an upper band edge of the bandgap at around $\omega\Lambda/c=13.30$. A bandgap in P1 to P6 is a range of frequencies of light for a given β. For the present examples, the bandgap is slightly wider than 0.35 (in units of $\omega\Lambda/c$). The inventors estimate that the minimum practical width for a PBG fibre bandgap would be around 0.05 in the present units of measure but, more preferably, would be greater than 0.1.

Modes that are between the light line and the lower band edge (that is, to the left of the light line) will concentrate in the glass and be evanescent in air whereas the modes that are between the light line and the upper band edge (that is, to the right of the light line) may be air-guiding.

As shown in P1, relating to S1, there are around three modes between the light line and the lower band edge and around nine modes between the light line and the upper band edge (taking the thicker spikes as two modes). It is clear that S1 supports a significant number of modes, some of which could be air-guiding; although, it is unlikely that all of these modes will be excited by a given light input. Analysis of the individual modes shown in the bandgap of P1 leads to a finding that the mode marked as F1 is an air-guiding mode, which most closely resembles the form of a fundamental mode in a typical standard optical fibre and supports the maximum amount of light in air. The mode is found to be degenerate, being one of a pair of very similar modes falling at about the same position in the bandgap.

As shown in P2, relating to S2, approximately two modes lie between the light line and the lower band edge and there are around twelve modes between the light line and the upper band edge. As with S1, S2 supports a significant number of modes, some of which could be air-guiding. The mode marked F2 in P2 is found to be a degenerate, air-guiding mode that most closely resembles the form of a fundamental mode in a typical standard optical fibre and supports the maximum amount of light in air.

The structural characteristics of S2 are not that different from those of S1; the only differences being the reduced boundary node sizes in S2 and omission of the beads. Notably, the core defect diameters of the two structures are the same. However, the mode spectra for the two structures are significantly different, there being more potentially-air-guiding modes supported by S2 but fewer modes that are evanescent in air.

As shown in P3, relating to S3, there are around three modes between the light line and the lower band edge and around thirteen modes between the light line and the upper band edge. Again, it is clear that S3 supports a significant number of modes, some of which could be air-guiding. The mode marked F3 in P3 is a degenerate, air-guiding mode that most

closely resembles the form of a fundamental mode in a typical standard optical fibre and supports the maximum amount of light in air.

Again, the structural characteristics of S3 are only subtly different from those of either S1 or S2, with the core defect diameters of all structures being the same. However, the mode spectrum for S3 is, once more, significantly different from the mode spectra of either S1 or S2.

As shown in P4, relating to S4, which is a nineteen-cell core defect structure, there are approximately two to four modes between the light line and the lower band edge and in excess of twenty modes between the light line and the upper band edge of the bandgap region. Clearly, S4 appears to support significantly more modes than any of the foregoing seven-cell core defect structures. The mode marked F4 in P4 is again a degenerate, air-guiding mode that most closely resembles the form of a fundamental mode in a typical standard optical fibre and supports the maximum amount of light in air.

The core defect diameter of S4 is significantly larger than in S1, whereas the other parameters are substantially the same. On the basis of prior art thinking it is not a surprise that there appear to be significantly more modes supported in the nineteen-cell core defect structure of S4 than in any of the seven-cell core defect structures S1 to S3.

As shown in P5, relating to S5, there are approximately four modes between the light line and the lower band edge and around fifteen to twenty modes between the light line and the upper band edge. Again, S5 appears to support significantly more modes than the foregoing seven-cell core defect structures. The mode marked F5 in P5 is a degenerate, air-guiding mode that most closely resembles the form of a fundamental mode in a typical standard optical fibre and supports the maximum amount of light in air.

The mode spectra for S4 and S5 are similar in terms of numbers of modes, with both structures supporting a number of evanescent and possibly air-guiding modes.

As shown in P6, relating to S6, there is a single mode between the light line and the lower band edge and approximately twelve to fifteen modes between the light line and the upper band edge. Thus, S6 appears to support significantly fewer modes than either of S4 or S5, even though the core defect sizes are the same. Surprisingly, the mode spectrum of S6 appears to resemble, in both numbers and positions of modes, the mode spectrum of S2, which is a seven-cell core defect structure. This is contrary to prior art thinking, which indicates that larger core defects should support, proportionately, more modes. The mode marked F6 in P6 is again a degenerate, air-guiding mode that most closely resembles the form

of a fundamental mode in a typical standard optical fibre and supports the maximum amount of light in air.

On the basis of the above six examples of different PBG fibre structures, it is clear that the numbers and locations of modes in a mode spectrum are not determined only by size of the core defect, index difference between a core and cladding and wavelength of light; even when the cladding structure is fixed. Taking S1 to S3, for example, it is clear that the locations of modes and, in particular, the number of modes that are likely to be evanescent in air or possibly air-guiding, can be varied significantly by varying the node size, and presence or absence of beads, about the core defect boundary, without the need to vary the core defect size. Additionally, while certain PBG fibre structures that support a greater number of modes – especially potentially air-guiding modes – may be made by increasing the core defect size for any given cladding structure, it also appears possible to increase the core defect size without significantly increasing the number of modes that are supported by the structure. This is surprising and contrary to the thinking in the prior art.

Figure 7 comprises six plots, D1 to D6, which show the mode intensity distributions, over a transverse cross-section of a respective PBG fibre structure, for modes F1 to F6 respectively. The shading of the plots is inverted, such that darker areas represent more intense light than lighter regions. Each plot shows the position and orientation of x and y planes, which correspond to the x and y planes of the structures, as illustrated in Figures 3 and 4. These plots were produced using the results obtained by solving Maxwell's equations for each structure, as described above.

The graphs in Figures 8 and 9 show the mode intensity for modes F1 to F6 along longitudinal planes x and y of D1 to D6 respectively. The intensity values are normalised so that the maximum intensity of the mode is at 0dB on the graph; the y-axis scale being logarithmic. The shaded vertical lines and bands across the graphs coincide with and represent the glass regions of the actual respective structure along the x and y planes. For the x and y planes, therefore, it is possible to see how the light intensity of the mode varies in the air and glass, and across the glass/air boundaries, of each structure.

Table 1 below shows, for modes F1 to F6, the approximate normalised frequency at which the mode lies within the bandgap of its respective structure and the percentage of light that is in air rather than in the high index silica regions.

Mode Number	Normalised frequency ($\omega\Lambda/c$)	% light in air
F1	13.14	92.8
F2	13.12	97
F3	13.11	97.5
F4	13.05	97.7
F5	13.04	99.6
F6	13.04	99.5

Table 1

The percentage of light in air for modes is found by calculating the integral of the light intensity across only the air regions of the plots in Figure 7 and normalising to the total power. Of course, the plots in Figure 7 represent the intensity across only an inner region of the various PBG fibre structures. Accordingly, the respective percentages of light in air are calculated for the inner regions only and may be different if calculated across entire PBG fibre structures instead. However, as will be seen, the intensities have typically reduced so considerably towards the edges of the plots that any light in regions outside of the inner regions, whether in air, glass or both, is unlikely to have any impact on the percentage of light in air values.

Plot D1 shows the mode intensity distribution for the F1 mode, which was found at a normalised frequency $\omega\Lambda/c$ of about 13.14. Plot D1 together with graphs x1 and y1 show that the F1 mode has a generally round central region in the core defect. The central region of the mode is intense at its centre and decays sharply towards the core defect boundary. There are two intense satellites to the left and right of the central region, coincident with the core defect boundary, and a number of less intense satellites that form a broken ring around the central region. As shown in graph x1, the satellites to the left and right of the central region have slightly higher intensities than the maximum intensity of the central region. It is significant to note that these intense satellites, along with the larger ones of the less intense satellites around the boundary, appear to coincide with the beads of S1. In addition, it would appear that the remainder of the less intense satellites appear to coincide with the boundary nodes of S1. There is evidence in D1 of some light being concentrated further out from the centre of the structure than the core defect boundary although, as is supported by graphs x1 and y1, the light intensity drops-off rapidly away from the central region. The light that is outside the core defect appears to coincide with cladding nodes.

It is apparent that, for the seven-cell core defect structure S1, a significant amount of light concentrates in the pronounced beads. It is apparent, however, that the F1 mode is air-guiding, with a significant fraction of the light existing in the core defect and with a local intensity minimum of the mode falling within the core defect boundary. The intensity of the light in the glass of the cladding structure decreases significantly moving further away from the core defect boundary.

Plot D2 shows the mode intensity distribution of the F2 mode in the transverse plane of S2. The mode was found at a normalised frequency $\omega\Lambda/c$ of about 13.12. Plot D2 together with graphs x2 and y2 show that the F2 mode has a generally round central region in the core defect. The central region is intense at its centre and decays sharply towards the core defect boundary. There are six relatively lower intensity satellites about the central region, coincident with the core defect boundary, and lower intensity satellites in glass further out from the central region. The six satellites around the core defect boundary have a lower intensity than the maximum intensity of the central region, in contrast to the intense satellites of plot D1. It is believed that in plot D2 the intensities of the satellites around the core defect boundary are less than in plot D1 due to the removal of the pronounced beads; in-keeping with the observation that, for a seven-cell core defect structure, a significant amount of light concentrates in the pronounced beads.

As with the F1 mode, it is apparent that the F2 mode is air-guiding. It is also apparent that some of the light concentrates in the glass of the cladding structure.

The percentage of light in air for the F2 mode is 97%. This value is significantly larger than the value of 92.8% for the F1 mode even though the core defect size is the same. This increase in the amount of light in air is attributed to the reduction in diameter of the boundary nodes and omission of the beads. Accordingly, it is expected that S2 will have improved loss, non-linearity and mode coupling characteristics compared with S1.

Plot D3 shows the mode intensity distribution of the F3 mode in the transverse plane of S3. The mode was found at a normalised frequency $\omega\Lambda/c$ of about 13.11. The qualitative and quantitative characteristics of the F3 mode, as shown in plot D3 and graphs x3 and y3, very closely match those of the F2 mode. Similarly, the value of the percentage of light in air for the F3 mode is 97.5%, which is very close to the figure for the F2 mode. Accordingly, it is expected that S3 will also have improved loss, non-linearity and mode coupling characteristics compared with S1.

Plot D4 shows the mode intensity distribution of the F4 mode in the transverse plane of S4. The mode was found at a normalised frequency $\omega\Lambda/c$ of about 13.05. Plot D4 together with graphs x4 and y4 show that the F4 mode has a generally round central region in the core defect. The central region is intense at its centre and decays rapidly towards the core defect boundary, although not as rapidly as in Plots D1 to D3. The central region has a local minimum that falls close to and within the core defect boundary, which means that the central region of the mode in plot D4 has a diameter in the order of two pitches longer than for any of the seven-cell core defect structures.

There are a number of low intensity satellites around the central region in plot D4, which appear to coincide with the boundary nodes of S4. From graphs x4 and y4, these satellites appear to be more than 20dB lower than the peak intensity of the central region. However, it should be noted that the x4 plane does not cross the core defect boundary at a bead, whereas planes x1 to x3 do, which means it is not possible to make a direct comparison of satellite intensity between graph x4 and graphs x1 to x3. The fact that the satellites in plot D4 appear so faint, though, does indicate that they have a significantly reduced intensity compared with satellites in plots D1 to D3.

The F4 mode is apparently air-guiding, with a significant fraction of the light existing in the core defect. Light which is guided outside of the core defect is concentrated in the glass. The percentage of light in air for S4 is 97.7%. This value is an improvement over the highest seven-cell core defect structure value by a small margin (0.2%) and a significant improvement (4.9%) over S1, which has a similar boundary node configuration. Accordingly, it is expected that S4 will have improved loss, non-linearity and mode coupling characteristics compared with S1.

Plot D5 shows the mode intensity distribution of the F5 mode in the transverse plane of S5. The mode was found at a normalised frequency $\omega\Lambda/c$ of about 13.04. Plot D5 together with graphs x5 and y5 show that the F5 mode is very similar in form to the F4 mode, with an intense central region and only very faint satellites outside of the central region. These satellites appear fainter than those in plot D4. Like the F4 mode, it is apparent that the F5 mode is air-guiding with a significant fraction of the light existing in the core defect.

The percentage of light in air for the F5 mode is 99.6%, which is significantly higher than the value of 97.7% for the F4 mode, even though the core defect sizes are the same. This increase in light in air value is attributed to the reduction in size of the boundary nodes and omission of the beads in S5 when compared with S4. It is expected that S5 will have

significantly improved loss, non-linearity and mode coupling characteristics compared with S1 and S4.

Plot D6 shows the mode intensity distribution of the F6 mode in the transverse plane of S6. The mode was found at a normalised frequency $\omega\Lambda/c$ of about 13.04. Plot D6 together with graphs x6 and y6, relating to the F6 mode, very closely match the qualitative and quantitative characteristics of the F5 mode. In addition, the percentage of light in air for the F6 mode is 99.5%, which is similar to the value for the F5 mode. Accordingly, like S5, it is expected that S6 will have significantly improved loss, non-linearity and mode coupling characteristics compared with S1 and S4, while at the same time not supporting a significantly increased number of modes compared with the seven-cell core defect structures of Structures S1 to S3.

Table 2 below provides data for six further exemplary waveguide structures, S7 to S12. The waveguide structures for S7-S12 very closely resemble S3, in that the boundaries have no apparent beads and the boundary nodes have a similar diameter to those in S1. Due to the similarity, and for reasons of brevity herein, S7-S12 are not independently represented in the Figures. The difference between the structures is only in boundary vein thickness, as shown in Table 2. The variations in boundary vein thickness are compensated for by slight variations in core defect diameter.

Structure	Boundary Vein Width/Λ	Normalised frequency ($\omega\Lambda/c$)	% light in air
S7	0.0383	13.11	98.6
S8	0.0438	13.11 (13.29)	98.2 (97.7)
S9	0.0493	13.10	96
S10	0.0548	13.12 (13.28)	96.9 (98.3)
S11	0.0602	13.11	97.3
S12	0.0657	13.11	97.8

Table 2

In Table 2, boundary vein width is normalised relative to the pitch Λ of the structures, which was the same for each structure. Structure S10 has a boundary vein thickness the same as the cladding vein thickness and, hence, was closest in form to S3. For each structure, the position of the mode having the highest percentage of light in air is presented as a frequency that is normalised with respect to the pitch of the structure.

Discounting for the moment the values in parentheses in Table 2, the modes having the highest percentage of light in air for each structure were found to be ones which most closely resemble the fundamental mode in a standard optical fibre communications system. As can be seen, varying the width of the boundary veins has little effect on the position of the respective modes. In contrast, however, variation in boundary vein thickness has a significant impact on the percentage of light in air for the modes. Within the coarse range of boundary vein thicknesses examined, it can be seen that a candidate as a preferred structure in terms of maximum light in air is S7, which has a boundary vein thickness of around 0.0383Λ (around 70% of the cladding vein thickness). However, a significant improvement over S10 is also seen at a boundary vein thickness of around 0.0438Λ (around 80% of cladding vein thickness). It is worthy of note, also, that the improvement is not linear, with the boundary vein thickness of S9 (around 90% of cladding vein thickness) producing a lower percentage of light in air than either of S10 or S8. In addition, slight improvements over S10 are seen with S11 and S12, which have thicker boundary veins than S10.

Although not described herein in detail, the inventors have found that the mode spectra for structures S7 to S12 vary considerably with varying boundary vein thickness. The variations were at least as marked as those found by varying the boundary node size and bead presence in structures S1 to S3, which are very similar seven-cell core defect structures.

Turning now to the values in parentheses in Table 2, for structure S10, a mode having the values shown was found to be non-degenerate and to exist within the bandgap of S10 to the right of the light line. This mode was found to support the highest fraction of light in air for the structure.

All other modes, which have been shown herein to support the maximum fraction of light in air, have been degenerate.

The intensity distribution for the non-degenerate S10 mode is shown in Figure 10. As can be seen, the mode is characterised by two relatively more intense regions either side of the core defect centre and two relatively less intense regions, bridging the more intense regions, above and below the core defect centre, all within the core defect. There is clearly also some light in the cladding region.

As will be appreciated, a non-degenerate mode may find beneficial application, for example, in a system that is required to have minimal polarisation mode dispersion.

The mode represented by the values in parentheses for S8 was also found to be non-degenerate. However, for this structure, the value of percentage of light in air for this mode

was less than the value for the mode that most closely resembles the form of a fundamental mode.

It is expected that there are likely to be a number of non-degenerate modes supported by the present waveguide structures. However, whether or not the modes exist within the bandgap of a particular structure would depend on the relationship between the bandgap and the respective mode spectrum, which, as has been shown, can be extremely sensitive to core size and boundary form at least.

With reference to Figure 11, prior art structures of the kind exemplified by S1 may be made from a perform 1100 comprising a stack of hexagonal capillaries 1105. The hexagonal capillaries 1105 each have a circular bore. The cladding nodes 160 and boundary nodes 150 (from Figure 1) of the PBG fibre structure result from the significant volume of glass that is present in the perform 1100 wherever the corners 1110, 1115 of neighbouring capillaries meet. The beads 165 are formed from the glass of the inwardly-facing corners 1120 of the capillaries that bound an inner region 1125 of the pre-form 1100, which is to become the core defect region 110 of a PBG fibre structure. These corners 1120, and the two sides of each capillary that meet at the corners, recede due to surface tension as the stack of capillaries is heated and drawn. Such recession turns the two sides and the corner 1120 into a boundary vein 140, with a bead 165. The inner region 1125 may be formed by omitting the inner seven capillaries from the pre-form and, for example, supporting the outer capillaries using truncated capillaries at either end of the stack, as described in PCT/GB00/01249 (described above) or by etching away glass from inner capillaries in accordance with either PCT/GB00/01249 or US 6,444,133 mentioned above.

While it is possible to adapt the prior art processes in order to make the nineteen-cell core defect S4, which has beads on some of the boundary veins, the present inventors have appreciated that it would be more difficult to manufacture either of S5 or S6 using the prior art techniques. In particular, it would be difficult to control the diameters of boundary nodes using hexagonal cross section capillaries of the kind described with reference to Figure 11. On the other hand, it is difficult to make structures having cladding nodes with diameters which are significantly larger than their respective veins by using purely round capillaries, especially when the required AFF is high, for example higher than 75%.

Figure 12 illustrates one way of arranging a stack of capillaries 1200 to be drawn into a pre-form and fibre of the kind that is exemplified by S6. S6 has no apparent beads and the boundary nodes 150 are smaller in diameter than the cladding nodes 160. The cladding is

formed by stacking round cross section capillaries 1205 in a close-packed, triangular lattice arrangement. The cladding capillaries 1205 have an outer diameter of 1.04mm and a wall thickness of 40μm. The inner region 1210 of the stack contains a large diameter capillary 1215 having an outer diameter of 4.46mm and a wall thickness of 40μm. The large diameter capillary 1215 supports the cladding capillaries while the stack is being formed and eventually becomes part of the material that forms a core defect boundary 145.

Interstitial voids 1220 that form at the locus of each close-packed, triangular group of three cladding capillaries are each packed with a glass rod 1225, which has an outer diameter of 0.498mm. The rods 1225 are inserted into the voids 1220 after the capillaries have been stacked. The rods 1225 that are packed in voids 1220 assist in forming cladding nodes 160, which have a diameter that is significantly greater than the thickness of the veins that meet at the nodes. Omission of a rod from a void in the cladding would lead to the formation of a cladding node that has a significantly smaller diameter.

In order to avoid the formation of pronounced boundary nodes 150, which have a diameter that is significantly greater than the thickness of the respective nodes, the voids 1230 that are formed between the cladding capillaries 1205 and the large diameter capillary 1215 are not packed with rods, thereby minimising the volume of glass that is available, during drawing of the stack 1200, for formation of the boundary nodes 150. By design, the arrangement of capillaries and rods shown in Figure 12 does not lead to formation of beads.

The stack 1200 is arranged as described with reference to Figure 12 and is then over-clad with a further, relatively thick walled capillary (not shown), which is large enough to contain the stack and, at the same time, small enough to hold the capillaries and rods in place. The entire over-clad stack is then heated and drawn into a pre-form, during which time all the interstitial voids at the boundary, and remaining voids between the glass rods and the cladding capillaries, collapse due to surface tension. The pre-form is, again, over-clad with a final, thick silica cladding and is heated and drawn into optical fibre in a known way. If surface tension alone is insufficient to collapse the interstitial voids, a vacuum may be applied to the interstitial voids of the pre-form, for example according to the process described in WO 00/49436 (The University of Bath).

The diameters of the boundary nodes of a PBG fibre that would result from the stack in Figure 12, or a similar seven-cell core defect structure, may be further reduced by using a large diameter capillary 1215 having a thinner wall. A limiting factor in reducing the wall thickness would be the ability to make such a capillary.

Figures 15a and 15b are scanning electron micrographs showing a cross section of two different seven-cell core defect PBG fibres, made according to the preceding method. Both fibres are exemplary embodiments of the present invention and resemble structure S3. As can be seen, the fibre in Figure 15a has slightly thicker boundary and cladding veins than the fibre in Figure 15b. R for the fibre in Figure 15b is clearly larger than R for the fibre in Figure 15a. In other words, the cladding cells in Figure 15b are rounder than the cladding cells in Figure 15a. The core defect of the fibre in Figure 15b has a larger diameter than the core defect of the fibre in Figure 15a, even though both fibres have a seven-cell core defect. This is due to the core defect of the fibre in Figure 15b having been more highly pressurised during the drawing process than the core defect of the fibre in Figure 15a. One consequence of this is that the hexagonal boundary cells in Figure 15b are slightly squashed in the radial direction and expanded in the azimuthal direction, which causes a significant perturbation in the cladding structure to propagate radially outward from the centre of the core defect, compared with the structure in Figure 15a.

An alternative way to reduce the size of boundary nodes 150 is by omitting a large diameter capillary altogether. As illustrated in Figure 13, the stack of cladding capillaries 1305 and rods 1325 is supported around an insert 1315, for example made from graphite, platinum, tungsten or a ceramic material, which is in a central region 1310 of the stack and which has a higher melting point than silica glass and, preferably, a higher coefficient of thermal expansion. The stack 1300, including the insert 1315, is heated to allow the capillaries 1305 and rods 1325 to fuse into a pre-form. The pre-form is then allowed to cool and the insert 1315 is removed. It will be apparent that, at this point, the core defect would take on the hexagonal shape of the insert. An advantage of using an insert material having a higher coefficient of thermal expansion than silica is that, when the pre-form and insert 1315 are heated, the insert expands and increases the area of the central region 1310. When permitted to cool down again, the insert 1315 shrinks back down to its original size and the silica solidifies leaving an inner region that is larger than the insert. The insert, which as a result is loose-fitting in the central region, may then be removed readily from the pre-form with reduced risk of damaging or contaminating the pre-form. The resulting pre-form is then heated and drawn in the usual way to form a PBG fibre. During the drawing step, it will be appreciated that the corners of the hexagonal core defect will, by virtue of surface tension, retract and flatten off, leaving a twelve-sided core defect closely resembling that in structure

the inventors propose that given a cladding structure that provides a PBG and a core defect in the cladding structure that supports guided modes, the form of the boundary at the interface between the core defect and the cladding structure will have a significant impact on the characteristics of the waveguide, as described herein.

The skilled person will also appreciate that, regarding the exemplary PBG waveguide structures described hereinabove, some structures are embodiments of the present invention whereas other structures are not. The structures that are not embodiments of the present invention are included for comparison purposes in order to assist in demonstrating the differences in characteristics between different structures. Additionally, the skilled person will appreciate that the structures described herein fit on a continuum comprising a huge number of different structures, for example having different combinations of core defect size, boundary node size, boundary vein thickness and, in general, boundary and cladding form. Clearly, it would be impractical to illustrate each and every variant of PBG waveguide structure herein. As such, the skilled person will accept that the present invention is limited in scope only by the present claims.

S5. A similar procedure, using a smaller insert to form a seven-cell core defect pre-form, could be used to make a structure closely resembling structure S2.

On the basis of the foregoing discussion, it will be apparent to the skilled person that the use of an insert in the formation of a pre-form is not limited to formation of nineteen-cell core defect structures and could be applied to making pre-forms for other core defect sizes, for example one-cell, seven-cell or thirty-seven cell core defect structures. Indeed, all of these structures have a core defect notionally centred on a primitive unit cell. Of course, a structure could be made, which has a core defect centred on a notional node and which lies at the locus of three notional neighbouring primitive unit cells. For example, the core defect could be made by removing three primitive unit cells that are arranged in a regular triangle, or three primitive unit cells as well as the nine primitive unit cells around the three primitive unit cells, etc. Further, inserts having, for example, star-shaped, elongate, round, square, rectangular, elliptical or irregular cross sections, or any other practical shape for that matter, could be applied to making pre-forms for fibre structures. Additionally or alternatively, inserts could be made by combining plural pieces. For example, an insert could be 'stacked' into a pre-form 1400 using elongate members 1415 having similar cross sections to the capillaries, as shown in Figure 14. As such, the insert could be made to match the cladding very closely, which may prove advantageous.

A further alternative way to reduce the size of boundary nodes 150 is by using the process described in PCT/GB00/01249 (described above), wherein the inner capillaries are replaced by truncated capillaries, which support the outer capillaries at either end of the stack. The stack may be drawn to an optical fibre in the normal way, and the parts of the fibre incorporating the truncated capillary material may be discarded. In principle, truncated capillaries may also be used to support the stack part way along its length.

The skilled person will appreciate that the various structures described above may be manufactured using a manufacturing process described with reference to Figures 12-14 or one of the prior art processes. For example, rather than using a stacking and drawing approach to manufacture, a pre-form may be made using a known extrusion process and then that pre-form may be drawn into an optical fibre in the normal way.

In addition, the skilled person will appreciate that while the examples provided above relate exclusively to PBG fibre cladding structures comprising triangular arrays, the present invention is in no way limited to such cladding structures. For example, the invention could relate equally to square lattice structures, or structures that are not close-packed. In general,

CLAIMS

1. An optical waveguide, having a plane cross section and a length dimension, which extends perpendicular to the plane cross section, comprising:

a photonic bandgap structure for providing a photonic bandgap over a range of frequencies of light, the photonic bandgap structure comprising, in the plane cross section, an arrangement of relatively low refractive index regions interspersed with relatively high refractive index regions, which extend parallel to the length dimension;

a core defect comprising a region of relatively low refractive index, which extends parallel to the length dimension and through the photonic bandgap structure; and

a boundary at the interface between the core defect and the photonic bandgap structure, the boundary, in the plane cross section, comprising a plurality of relatively high refractive index boundary veins joined end-to-end around the boundary between boundary nodes, each boundary vein having a length l and a thickness t, at the mid-point along the length l, and being joined between a leading boundary node and a following boundary node, and each boundary node having a diameter and being joined between two boundary veins and to a relatively high refractive index region of the photonic bandgap structure, wherein, in the plane cross section, around the boundary:

$t < d_L$ and $t < d_F$ is true for more than half of the boundary veins; and

$l \geq x(d_L+d_F)$ is true for at least one boundary vein,

where $x \geq 0.6$ and d_L, d_F are the diameters of the leading and following nodes respectively for each vein.

2. The waveguide according to claim 1, wherein $l \geq x(d_L+d_F)$ is true for a plurality of the boundary veins.

3. The waveguide according to claim 1 or claim 2, wherein $l \geq x(d_L+d_F)$ is true for at least half of the boundary veins.

4. The waveguide according to any one of the preceding claims, wherein $l \geq x(d_L+d_F)$ is true for all of the boundary veins.

5. The waveguide according to any one of the preceding claims, wherein $x \geq 0.8$.

6. The waveguide according to any one of the preceding claims, wherein $x \geq 1$.

7. The waveguide according to any one of the preceding claims, wherein, in the plane cross section, the thinnest point along at least some of the boundary veins is substantially at the mid-point.

8. The waveguide according to any one of the preceding claims, wherein, in the plane cross section, the thinnest point along each boundary vein is substantially at the mid-point.

9. The waveguide according to any one of the preceding claims, wherein, in the plane cross section, the photonic bandgap structure comprises an array of relatively low refractive index regions being separated from one another by relatively high refractive index regions.

10. The waveguide according to claim 9, wherein the array is substantially periodic.

11. The waveguide according to claim 9 or claim 10, wherein the array has a characteristic primitive unit cell and a pitch Λ.

12. The waveguide according to any one of claims 9 to 11, wherein the array is a substantially triangular array.

13. The waveguide according to claim 11 or claim 12, wherein, in the plane cross section, the thickness at the midpoint of a plurality of the boundary veins is less than 0.1Λ.

14. The waveguide according to any one of claims 11 to 13, wherein, in the plane cross section, the thickness at the mid-point of a plurality of the boundary veins is less than 0.049Λ.

15. The waveguide according to any one of the preceding claims, wherein, in the plane cross section, the relatively low refractive index regions in the photonic bandgap structure are separated from one another by relatively high refractive index veins that are joined at nodes, each node having a diameter and each vein having a length and a thickness at the mid-point along the length and being joined at each end to a node.

16. The waveguide according to claim 15, wherein, in the plane cross section, at least some boundary nodes have diameters that are significantly smaller than at least some nodes in the photonic bandgap structure.

17. The waveguide according to claim 15 or claim 16, wherein, in the plane cross section, substantially all boundary nodes have diameters that are significantly smaller than at least some nodes in the photonic bandgap structure.

18. The waveguide according to any one of claims 15 or claim 17, wherein, in the plane cross section, substantially all boundary nodes have diameters that are significantly smaller than a significant proportion of all nodes in the photonic bandgap structure.

19. The waveguide according to any one of claims 15 to 18, wherein, in the plane cross section, diameters of at least some of the nodes within the photonic bandgap structure are significantly larger than the mid-point thickness of the veins that are joined to the respective nodes.

20. The waveguide according to any one of claims 15 or claim 19, wherein, in the plane cross section, a significant proportion of all nodes within the photonic bandgap structure have diameters that are significantly larger than the mid-point thickness of the veins that are joined to the respective nodes.

21. The waveguide according to claim 19 or claim 20, wherein, said nodes in the photonic bandgap structure, which have a significantly larger diameter than the mid-point thickness of the veins that are joined to the nodes, have a diameter which is at least 1.5 times the thickness of the veins.

22. The waveguide according to any one of claims 19 to 21, wherein, said nodes in the photonic bandgap structure, which have a significantly larger diameter than the thickness of the veins that are joined to the nodes, have a diameter which is at least twice the thickness of the veins.

23. The waveguide according to any one of the preceding claims, wherein at least some of the relatively low refractive index regions are voids filled with air or under vacuum.

24. The waveguide according to any one of the preceding claims, wherein at least some of the relatively low refractive index regions are voids filled with a gas other than air or a liquid.

25. The waveguide according to any one of the preceding claims, wherein at least some of the relatively high refractive index regions comprise silica glass.

26. The waveguide according to any one of the preceding claims, wherein the proportion by volume of relatively low refractive index regions in the photonic bandgap structure is higher than 75%.

27. The waveguide according to any one of the preceding claims, wherein the proportion by volume of relatively low refractive index regions in the photonic bandgap structure is higher than 85%.

28. The waveguide according to any one of the preceding claims, wherein the proportion by volume of relatively low refractive index regions in the photonic bandgap structure is around 87.5%.

29. The waveguide according to any one of the preceding claims, which supports a mode having more than 90% of the mode power in relatively low refractive index regions.

30. The waveguide according to any one of the preceding claims, which supports a mode having more than 95% of the mode power in relatively low refractive index regions.

31. The waveguide according to any one of the preceding claims, which supports a mode having more than 98% of the mode power in relatively low refractive index regions.

32. The waveguide according to any one of the preceding claims, which supports a mode having more than 99% of the mode power in relatively low refractive index regions.

33. The waveguide according to any one of the preceding claims, which supports a mode having a mode profile that closely resembles the fundamental mode of a standard optical fibre.

34. The waveguide according to any one of the preceding claims, which supports a non-degenerate mode.

35. The waveguide according to claim 33 or claim 34, wherein said mode supports a maximum amount of the mode power in relatively low refractive index regions compared with other modes that are supported by the waveguide.

36. The waveguide according to any one of the preceding claims, wherein at least some of the boundary veins are substantially straight.

37. The waveguide according to any one of the preceding claims, wherein at least some of the boundary veins are bowed outwardly from the core defect.

38. An optical fibre comprising a waveguide according to any one of the preceding claims.

39. A transmission line for carrying data between a transmitter and a receiver, the transmission line including along at least part of its length a fibre according to claim 37.

40. A method of forming a photonic bandgap optical waveguide having a plane cross section and a length dimension, which extends perpendicular to the plane cross section, comprising the steps:

forming a preform stack by stacking a plurality of elongate elements;

omitting, or substantially removing at least one elongate element from an inner region of the stack; and

heating and drawing the stack, in one or more steps, into a photonic bandgap optical waveguide,

characterised by a photonic bandgap structure, a core defect and a boundary at the interface between the core defect and the photonic bandgap structure,

the photonic bandgap structure for providing a photonic bandgap over a range of frequencies of light, the photonic bandgap structure comprising, in the plane cross section, an arrangement of relatively low refractive index regions interspersed with relatively high refractive index regions, which extend parallel to the length dimension,

the core defect comprising a region of relatively low refractive index, which extends parallel to the length dimension and through the photonic bandgap structure,

the boundary at the interface between the core defect and the photonic bandgap structure, the boundary, in the plane cross section, comprising a plurality of relatively high refractive index boundary veins joined end-to-end around the boundary between boundary nodes, each boundary vein having a length l and a thickness t, at the mid-point along the length l, and being joined between a leading boundary node and a following boundary node, and each boundary node having a diameter and being joined between two boundary veins and to a relatively high refractive index region of the photonic bandgap structure, wherein, in the plane cross section, around the boundary:

$t < d_L$ and $t < d_F$ is true for more than half of the boundary veins; and

$l \geq x(d_L+d_F)$ is true for at least one boundary vein,

where $x \geq 2$ and d_L, d_F are the diameters of the leading and following nodes respectively for each vein.

41. The method according to claim 40, wherein the preform stack comprises a substantially periodic, triangular array of elongate elements.

42. The method according to claim 40 or claim 41, wherein the elements have a generally hexagonal transverse cross section.

43. The method according to claim 40 or claim 41, wherein the elements have a generally circular transverse cross section.

44. The method according to claim 43, wherein first elongate interstitial voids are formed between elements.

45. The method according to claim 44, including the additional step of introducing elongate elements into at least some of the first interstitial voids.

46. The method according to claim 45, wherein at least some of the elongate elements comprise rods.

47. The method according to claim 45, wherein at least some of the elongate elements comprise capillaries.

48. The method according to any one of claims 44 to 47, wherein elongate elements are introduced into substantially all of the first interstitial voids.

49. The method according to any one of claims 40 to 48, including the additional step of introducing a further elongate element into the inner region to support the elements around the inner region.

50. The method according to claim 49, wherein second interstitial voids are formed between the elements around the inner region and the further elongate element.

51. The method according to claim 50, including the additional step of introducing elongate elements into at least some of the second interstitial voids.

52. The method according to claim 51, wherein at least some of the elongate elements comprise rods.

53. The method according to claim 51, wherein at least some of the elongate elements comprise capillaries.

54. The method according to any one of claims 51 to 53, wherein a reduced fraction of the rods are introduced into the second interstitial voids compared with the number of rods that are introduced into a similar configuration of first interstitial voids.

55. A method according to claim 50, wherein no elongate elements are introduced into the second interstitial voids.

56. A method according to any one of claims 51 to 54, wherein at least some of the elongate elements that are introduced into the second interstitial voids have a smaller cross sectional area than the elongate elements that are introduced into the first interstitial voids.

57. The method according to any one of claims 49 to 56, wherein the further elongate element has a relatively low refractive index elongate inner region enclosed by a relatively high refractive index outer region, which becomes part of the photonic bandgap optical waveguide.

58. The method according to any one of claims 49 to 56, wherein the further elongate element comprises a material that has higher melting point and coefficient of thermal expansion than the relatively high refractive index material in the elongate elements.

59. The method according to claim 58, further comprising the steps of:

heating the preform stack in order to fuse the elongate elements around the further elongate element;

cooling the preform stack; and

removing the further elongate element from the preform stack prior to heating and drawing the preform stack.

60. The method according to any one of claims 40 to 59, wherein at least some of the relatively low refractive index regions comprise air or are under vacuum.

61. The method according to any one of claims 40 to 60, wherein at least some of the relatively low refractive index regions are voids filled with a gas other than air or a liquid.

62. The method according to any one of claims 40 to 61, wherein at least some of the relatively high refractive index regions comprise silica glass.

63. An optical fibre comprising a photonic bandgap optical waveguide made by the method of any one of claims 40 to 62.

64. A method of forming a photonic bandgap optical waveguide comprising the steps:

forming a preform stack by stacking relatively large circular cross section tubes into a triangular array of tubes, the stack of tubes comprising interstitial voids into which are placed relatively small cross section rods, which are sufficiently large to fill a significant portion of said voids;

omitting, or substantially removing, at least one relatively large circular cross section tube, and at least some rods that would have been adjacent the or each tube, from an inner region of the stack; and

heating and drawing the stack, in one or more steps, into a photonic bandgap optical waveguide, characterised by a photonic bandgap structure that surrounds a core defect and a boundary at the interface between the core defect and the photonic bandgap structure.

65. An optical waveguide comprising:

a photonic bandgap structure for providing a photonic bandgap over a range of frequencies of light, the photonic bandgap structure comprising, in the plane cross section, an arrangement of relatively low refractive index regions interspersed with relatively high refractive index regions, which extend parallel to the length dimension;

a core defect comprising a region of relatively low refractive index, which extends parallel to the length dimension and through the photonic bandgap structure; and

a boundary at the interface between the core defect and the photonic bandgap structure, the boundary, in the plane cross section, comprising a plurality of relatively high refractive index boundary veins joined end-to-end around the boundary between boundary nodes, each boundary vein having a length and a thickness, at the mid-point along the length, and being joined between a leading boundary node and a following boundary node, and each boundary node having a diameter and being joined between two boundary veins and to a relatively high refractive index region of the photonic bandgap structure, wherein, in the plane cross section, around the boundary, the waveguide supports a light mode in which at least 90% of the power of the mode is guided in relatively low refractive index regions of the waveguide.

66. An optical waveguide substantially as hereinbefore described, with reference to the accompanying drawings.

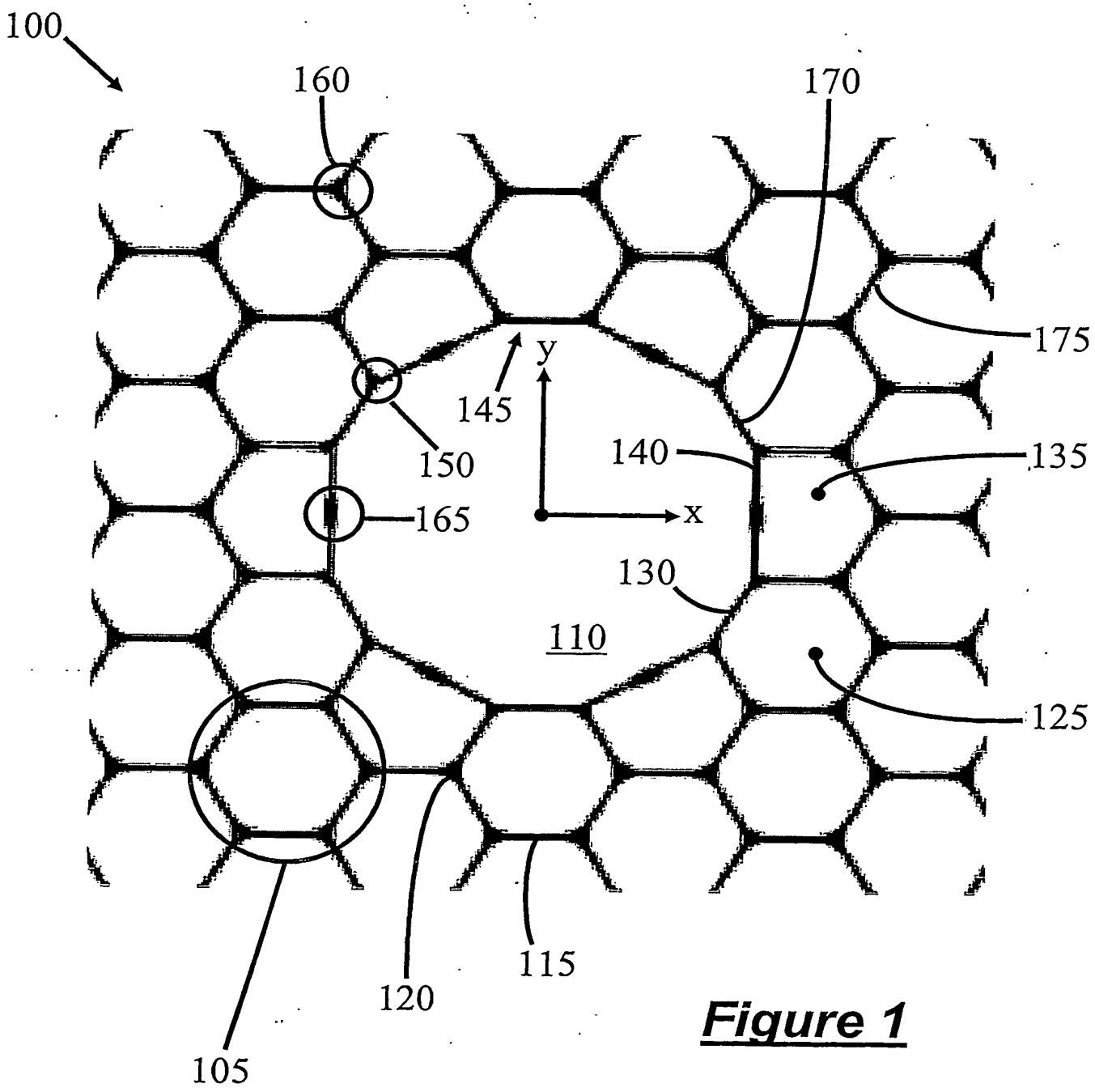

Figure 1

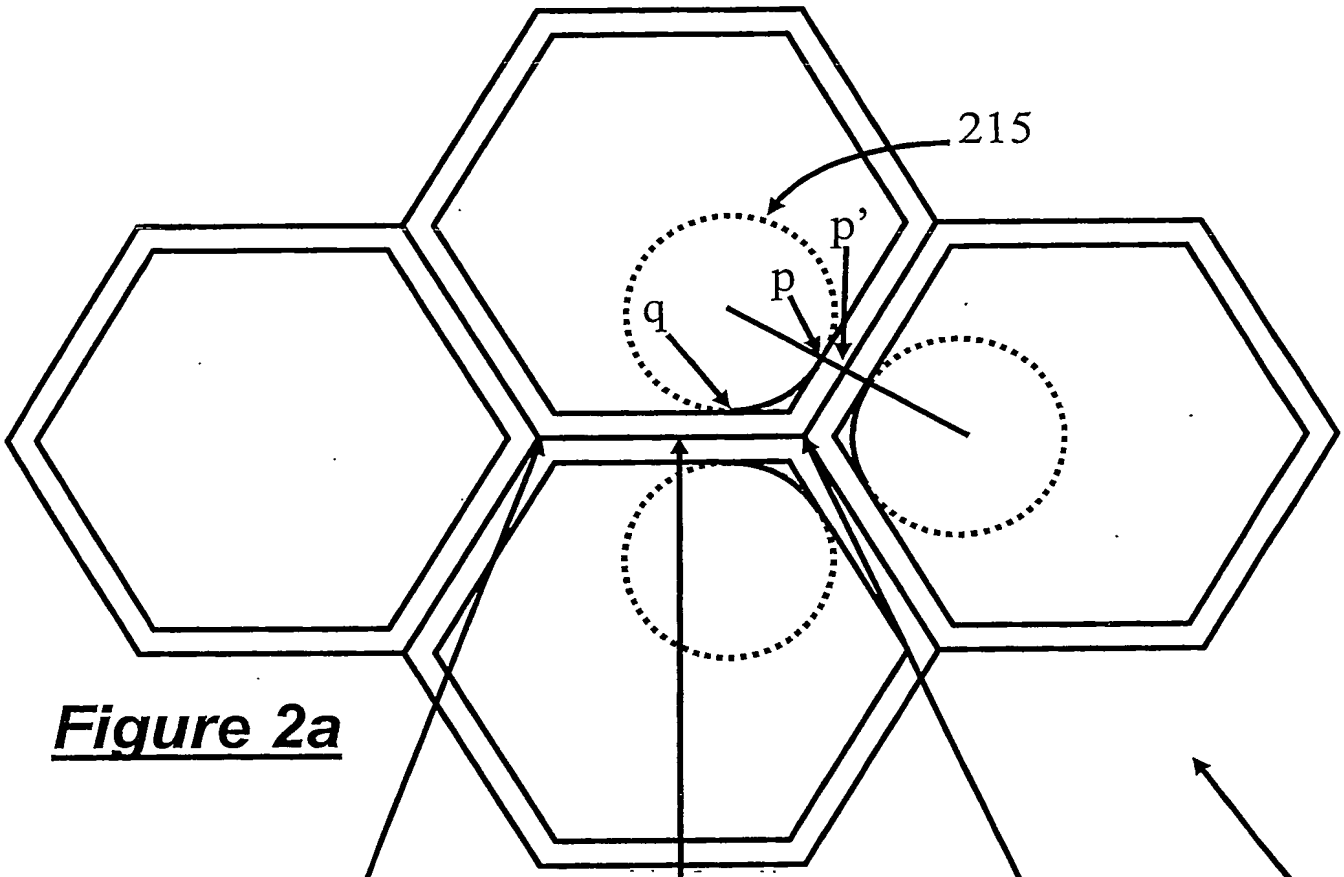

Figure 2a

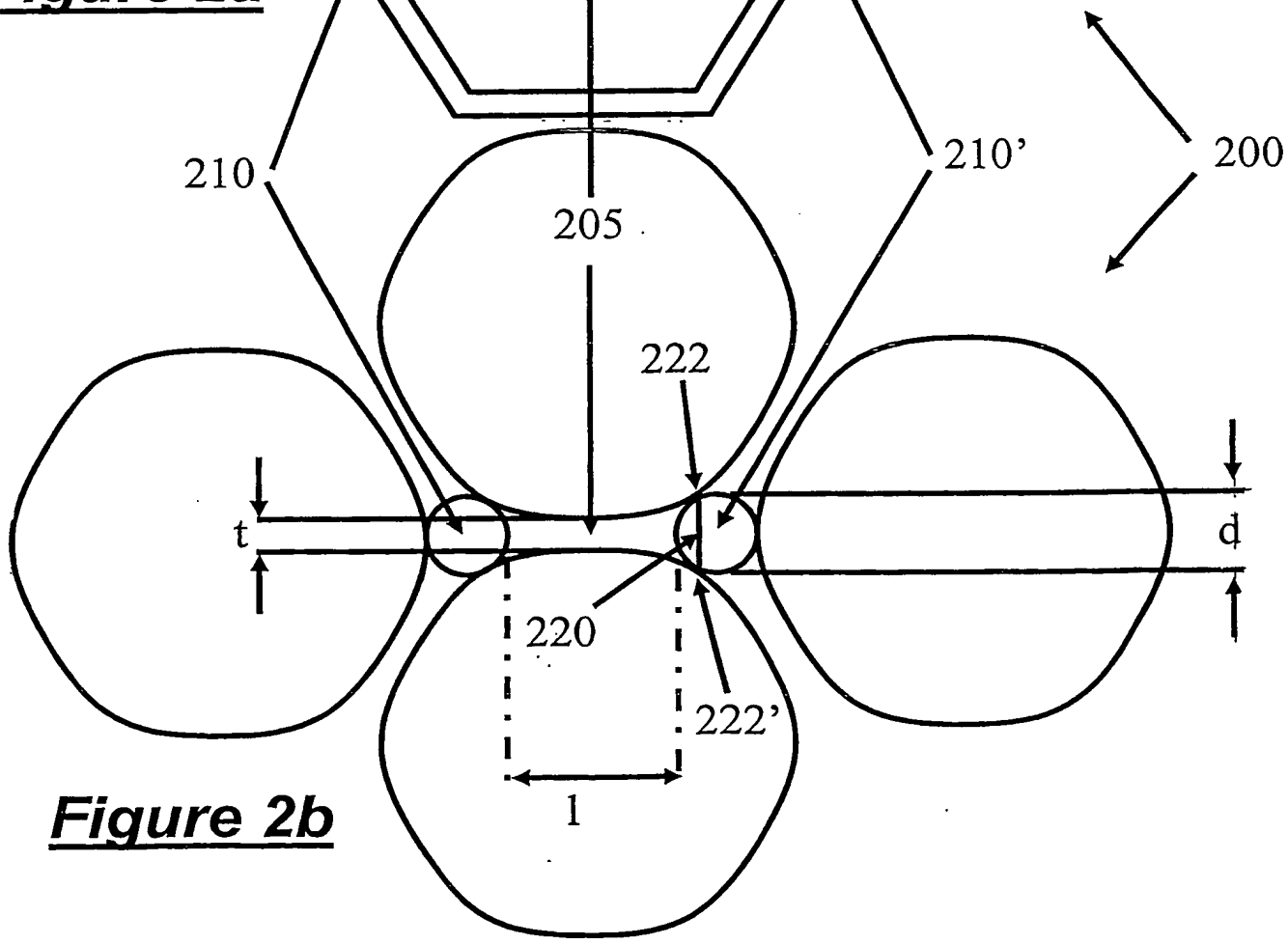

Figure 2b

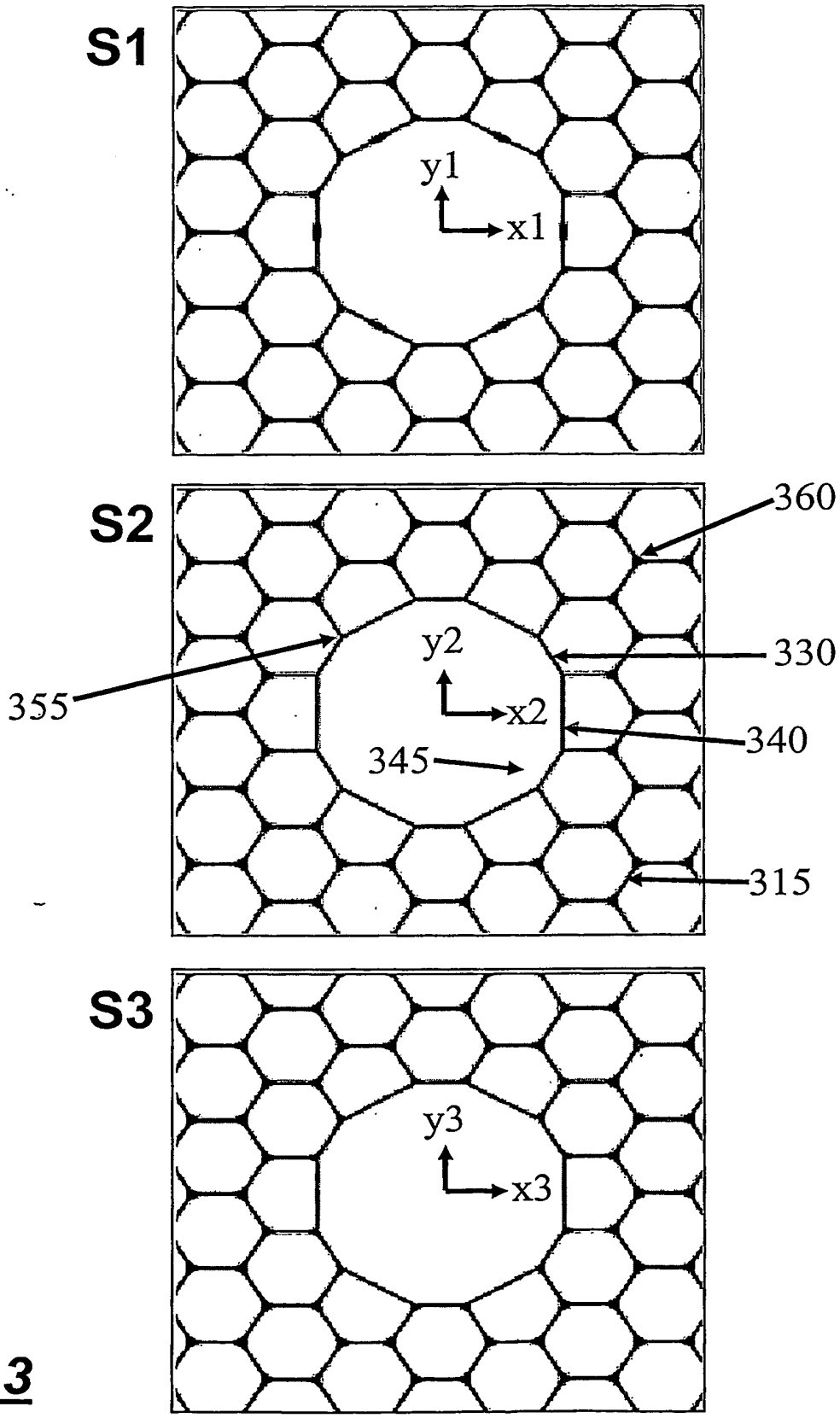

Figure 3

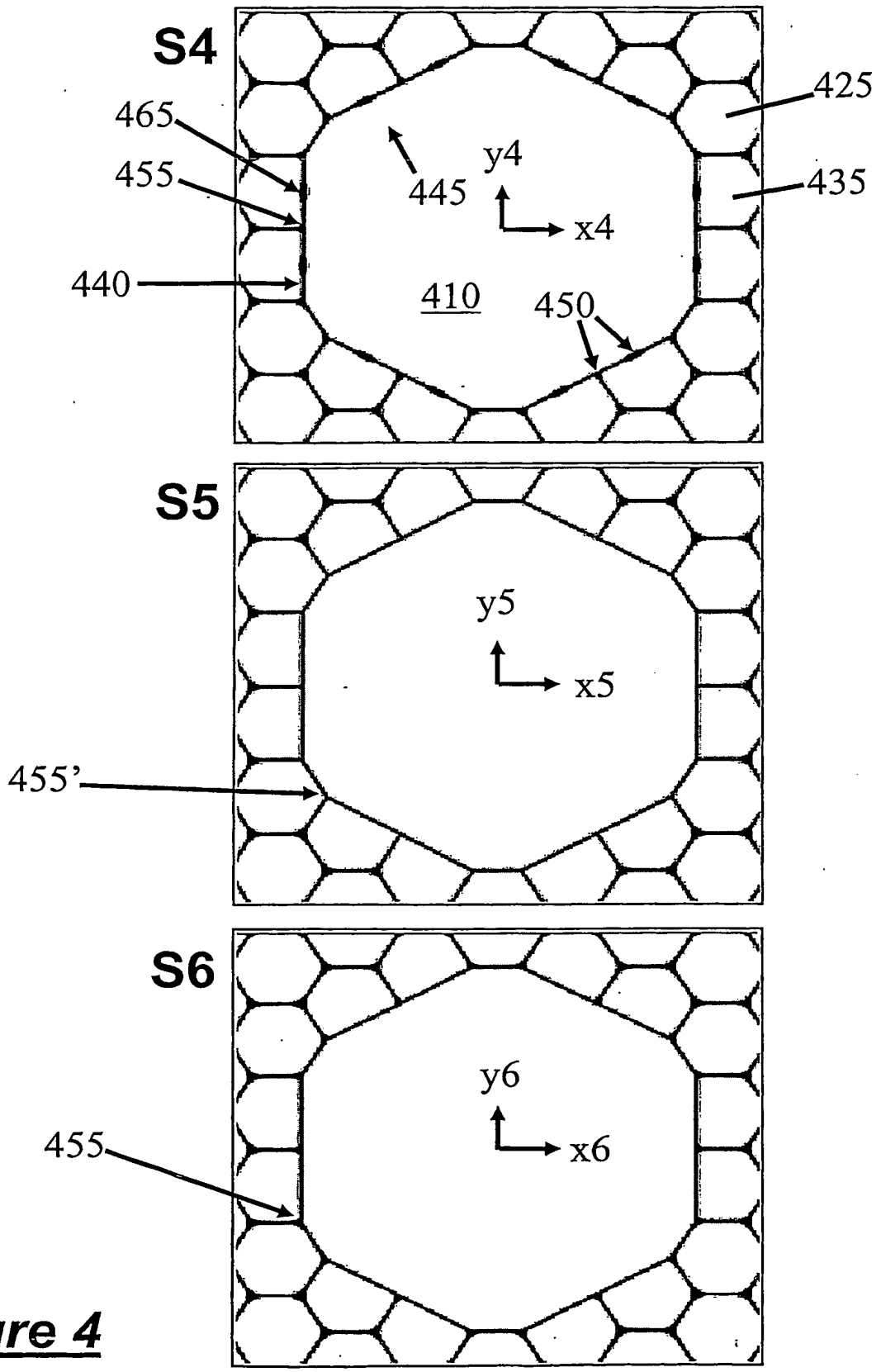

Figure 4

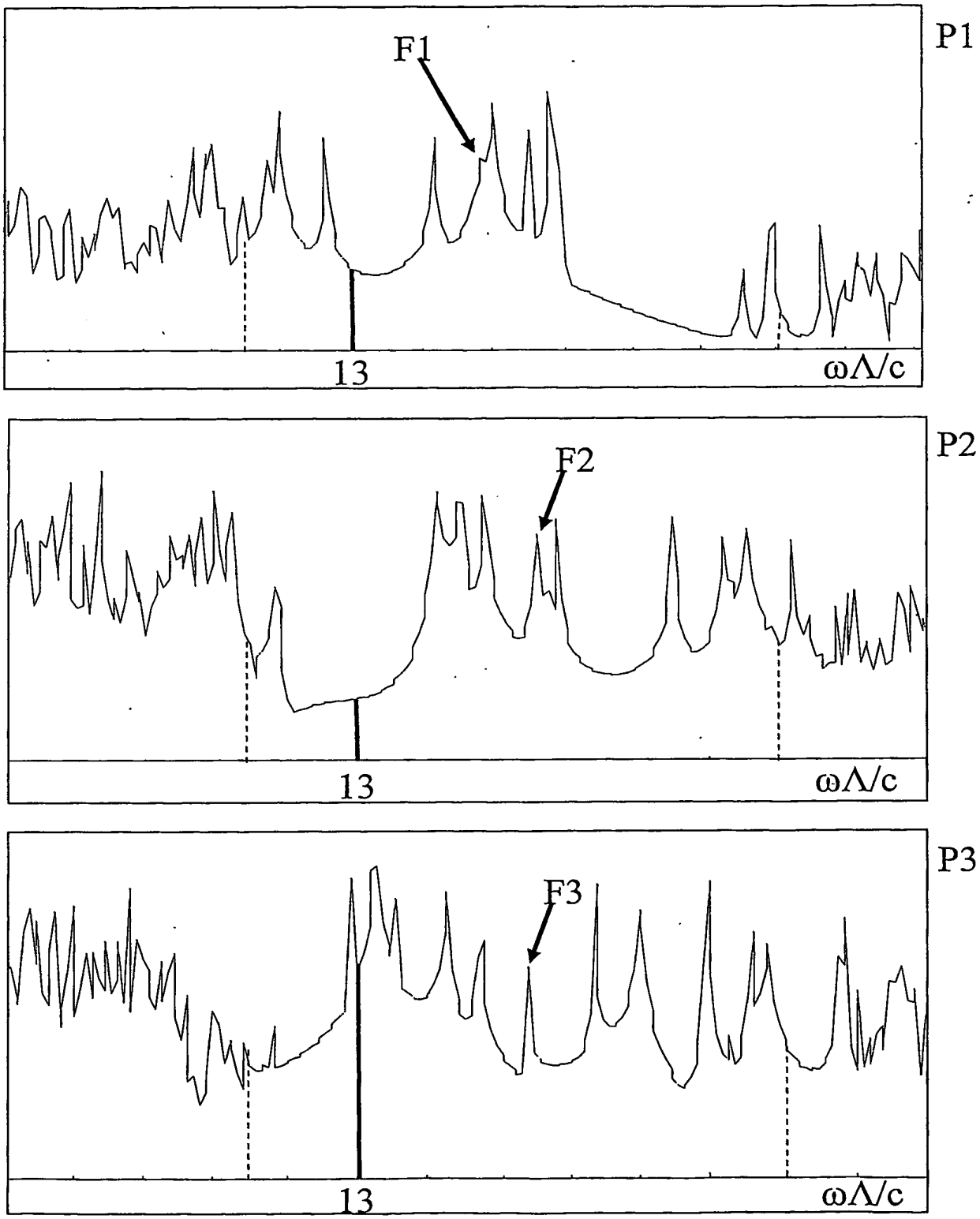

Figure 5

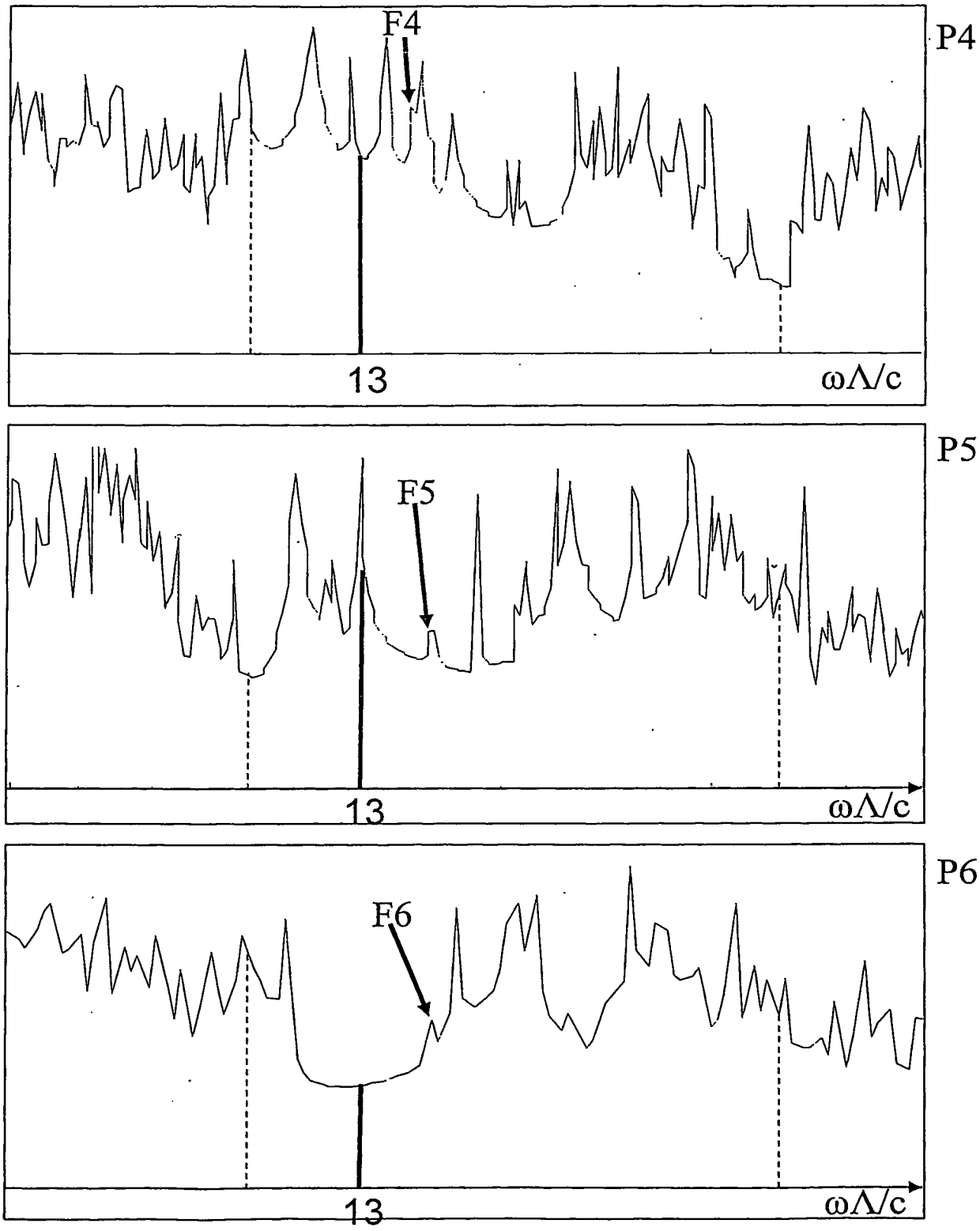

Figure 6

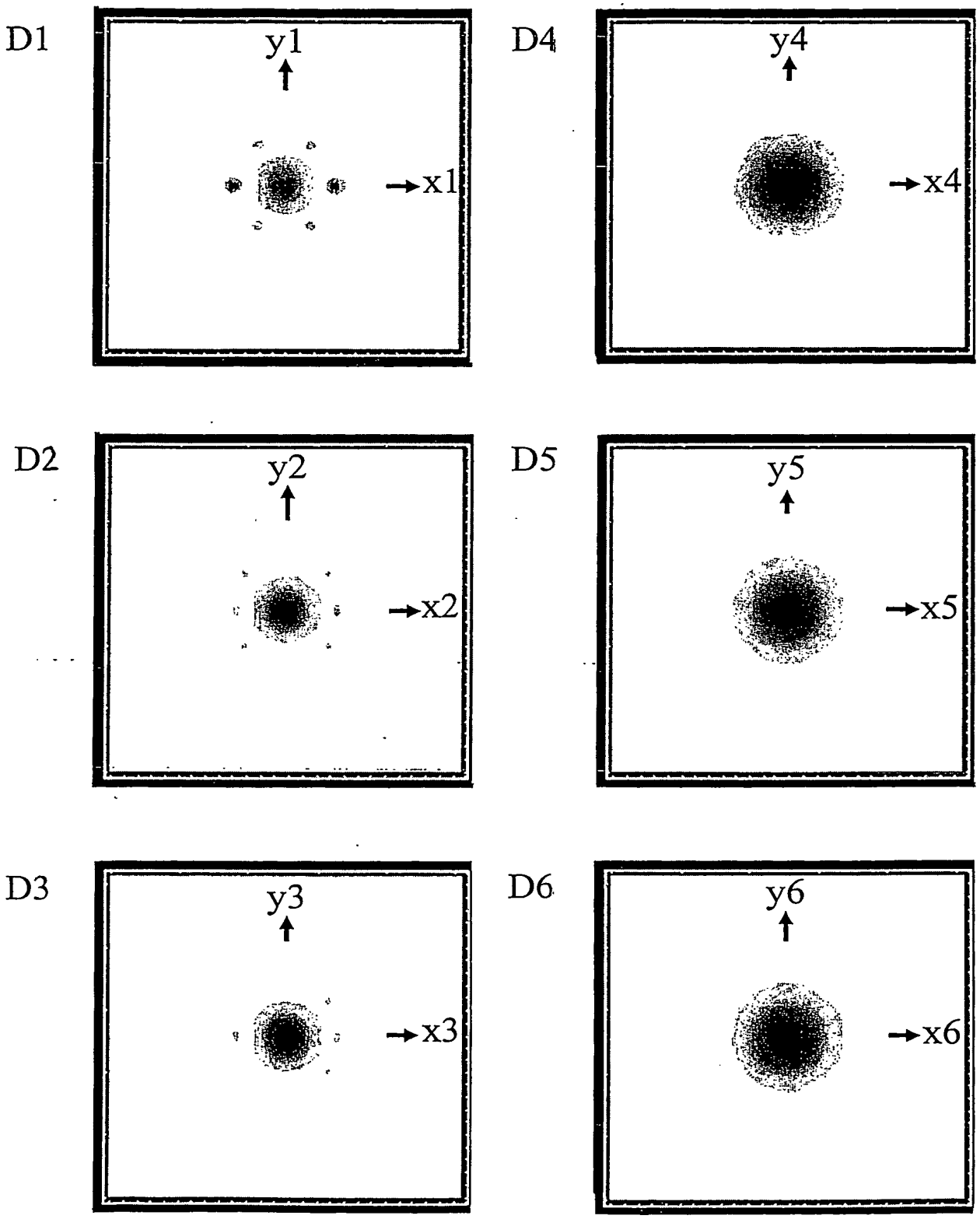

Figure 7

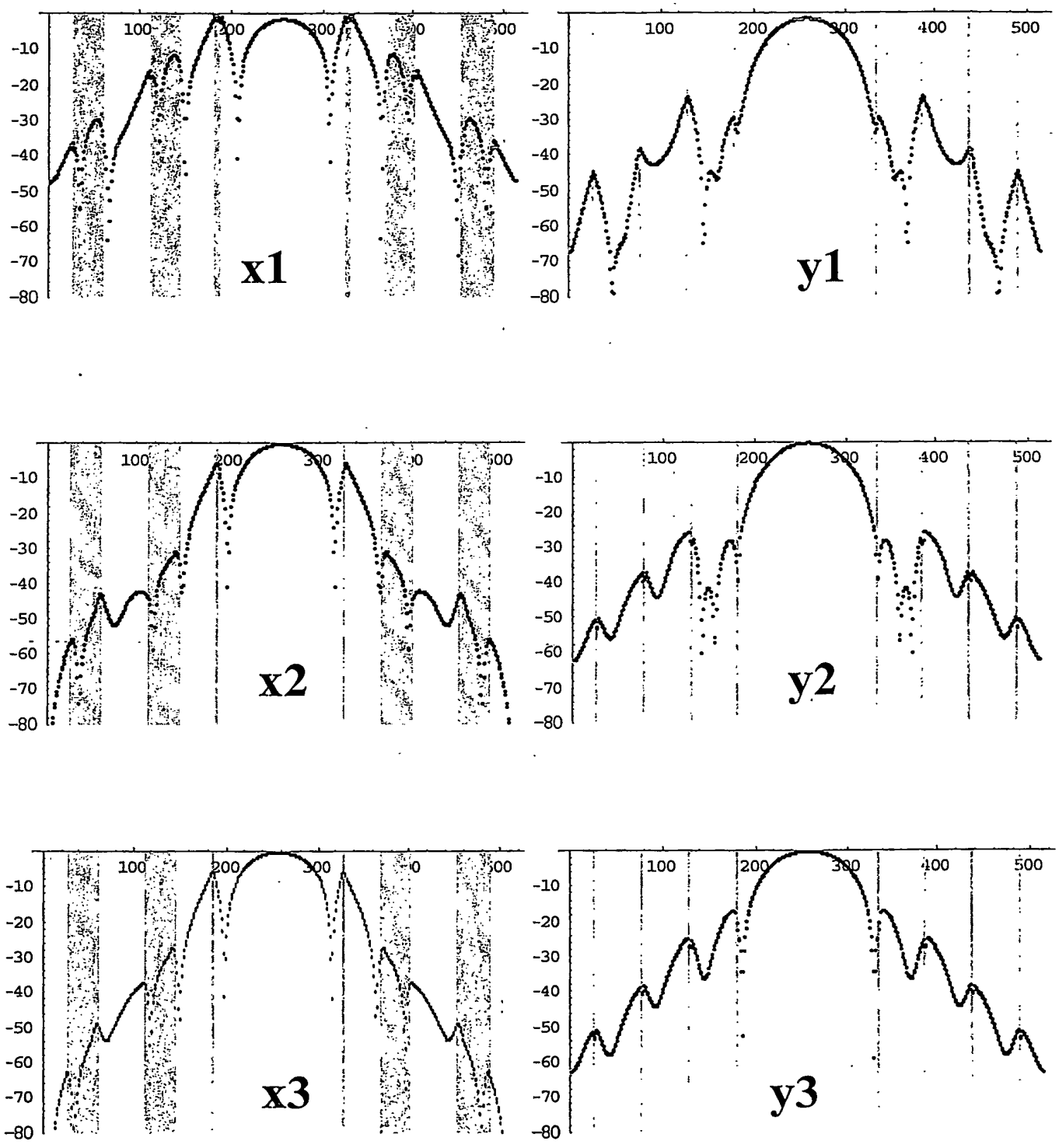

Figure 8

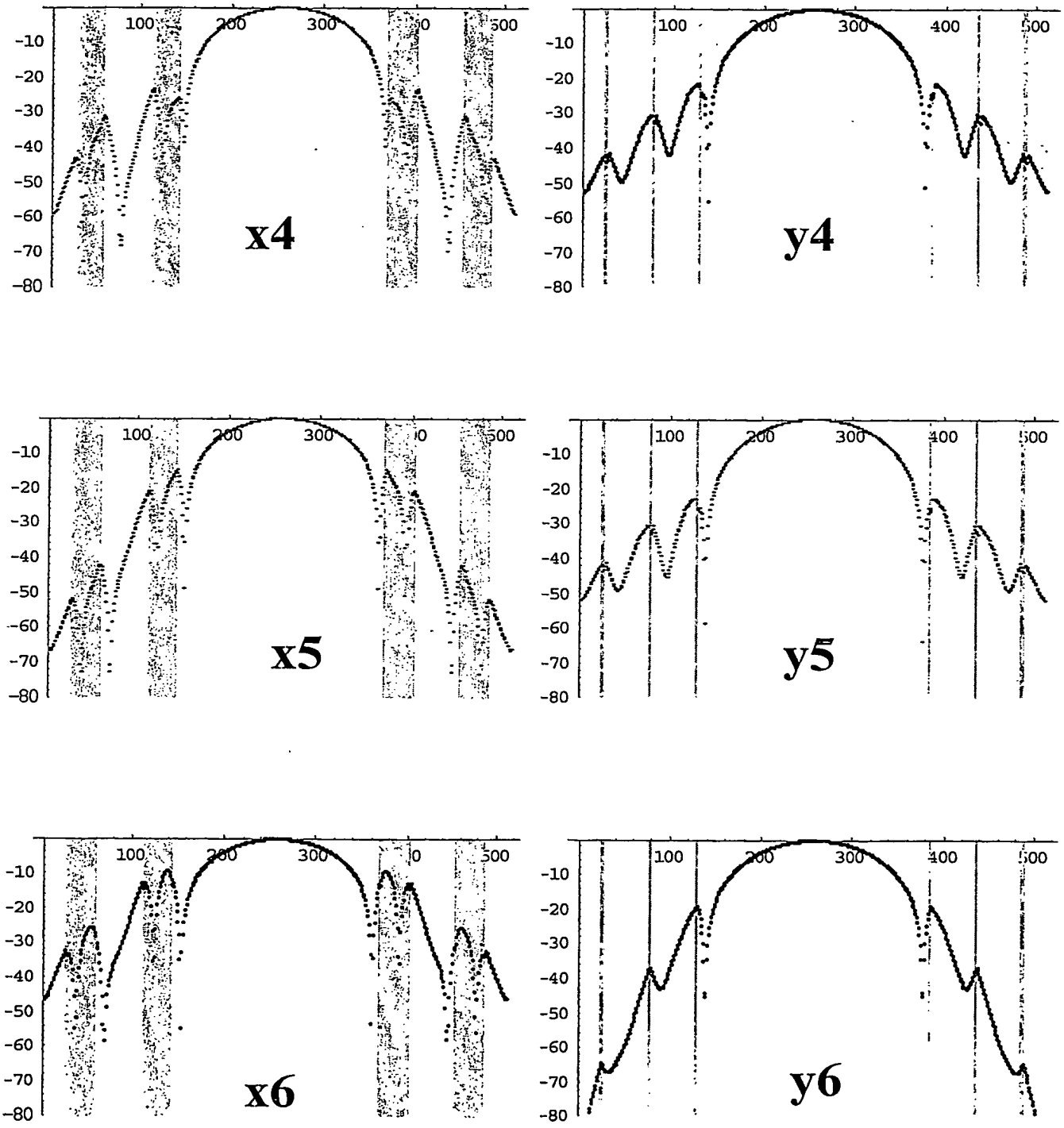

Figure 9

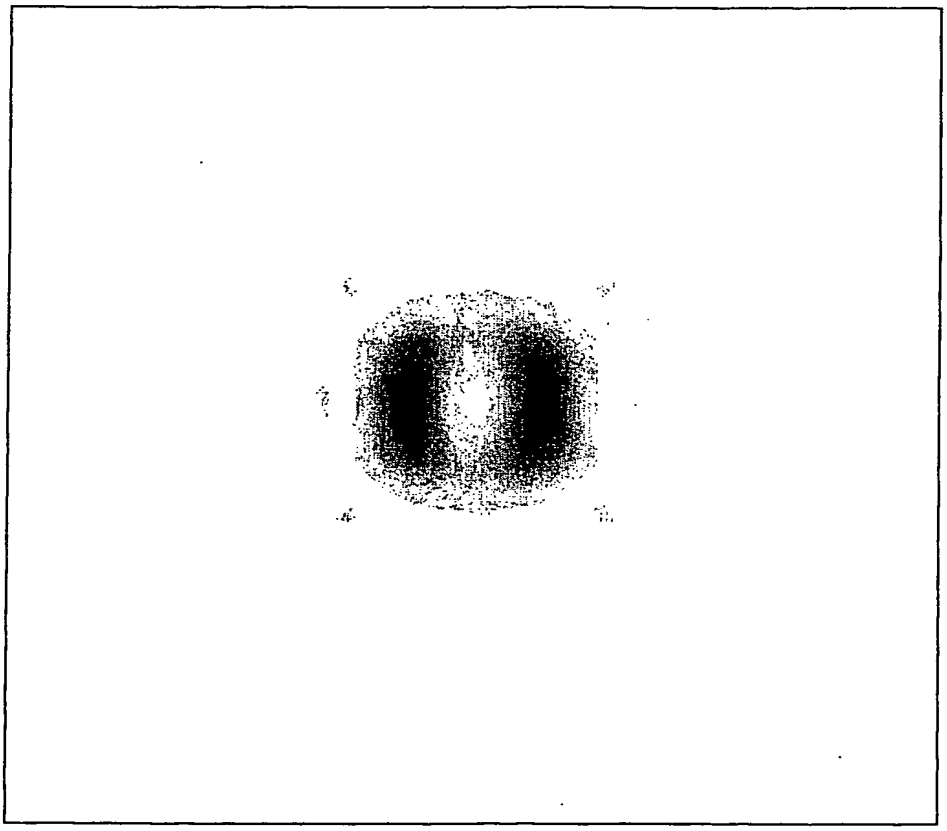

Figure 10

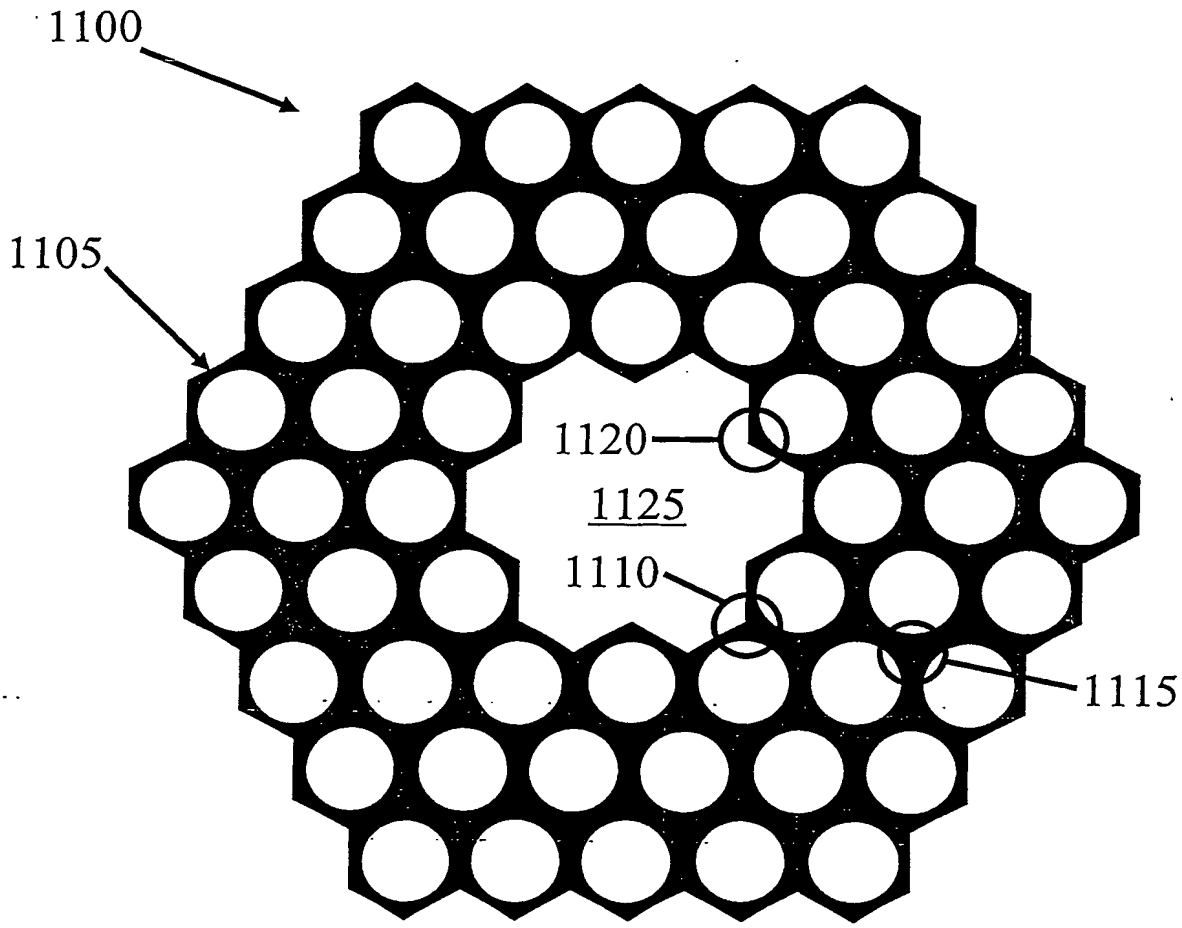

Figure 11

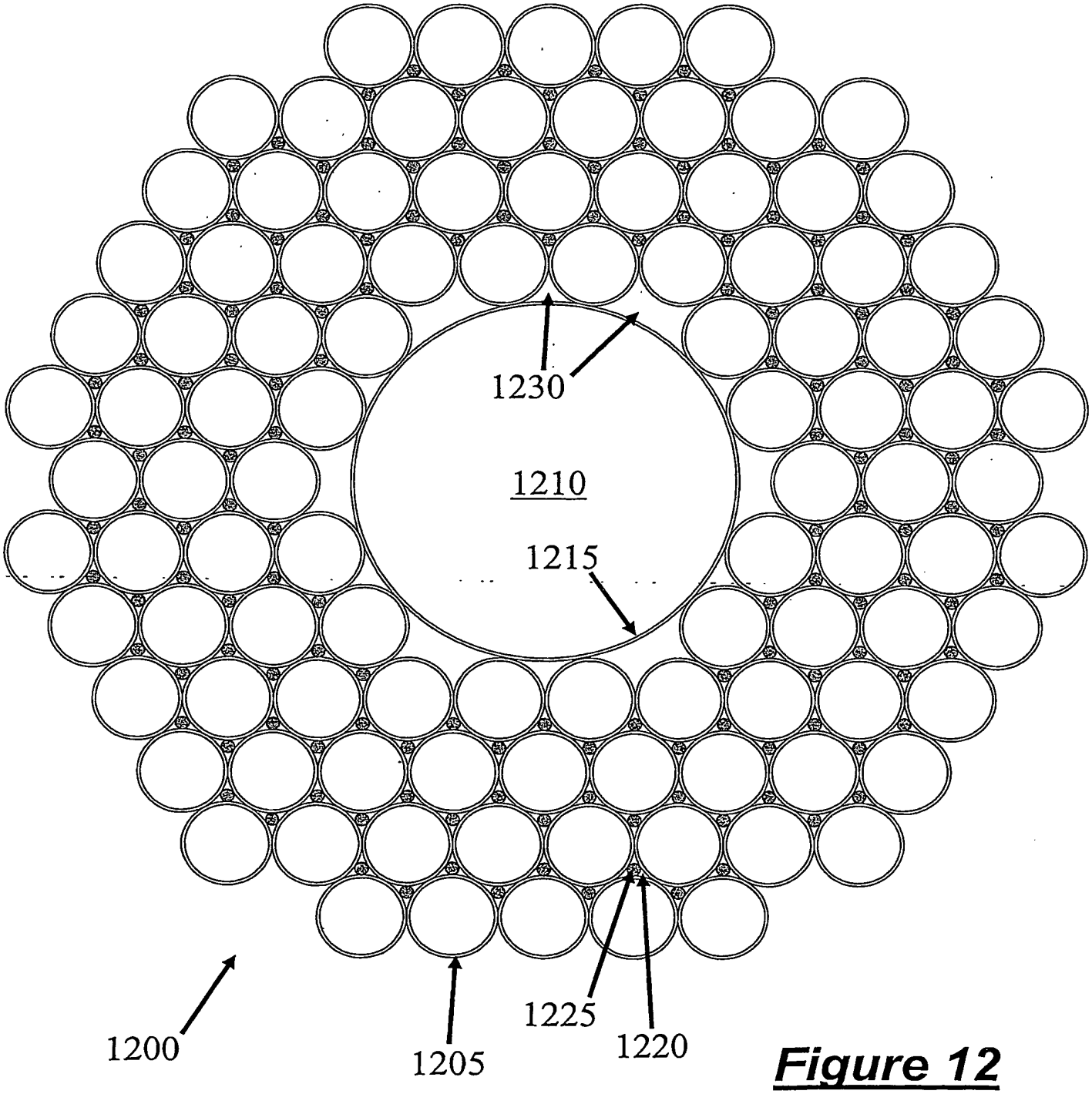

Figure 12

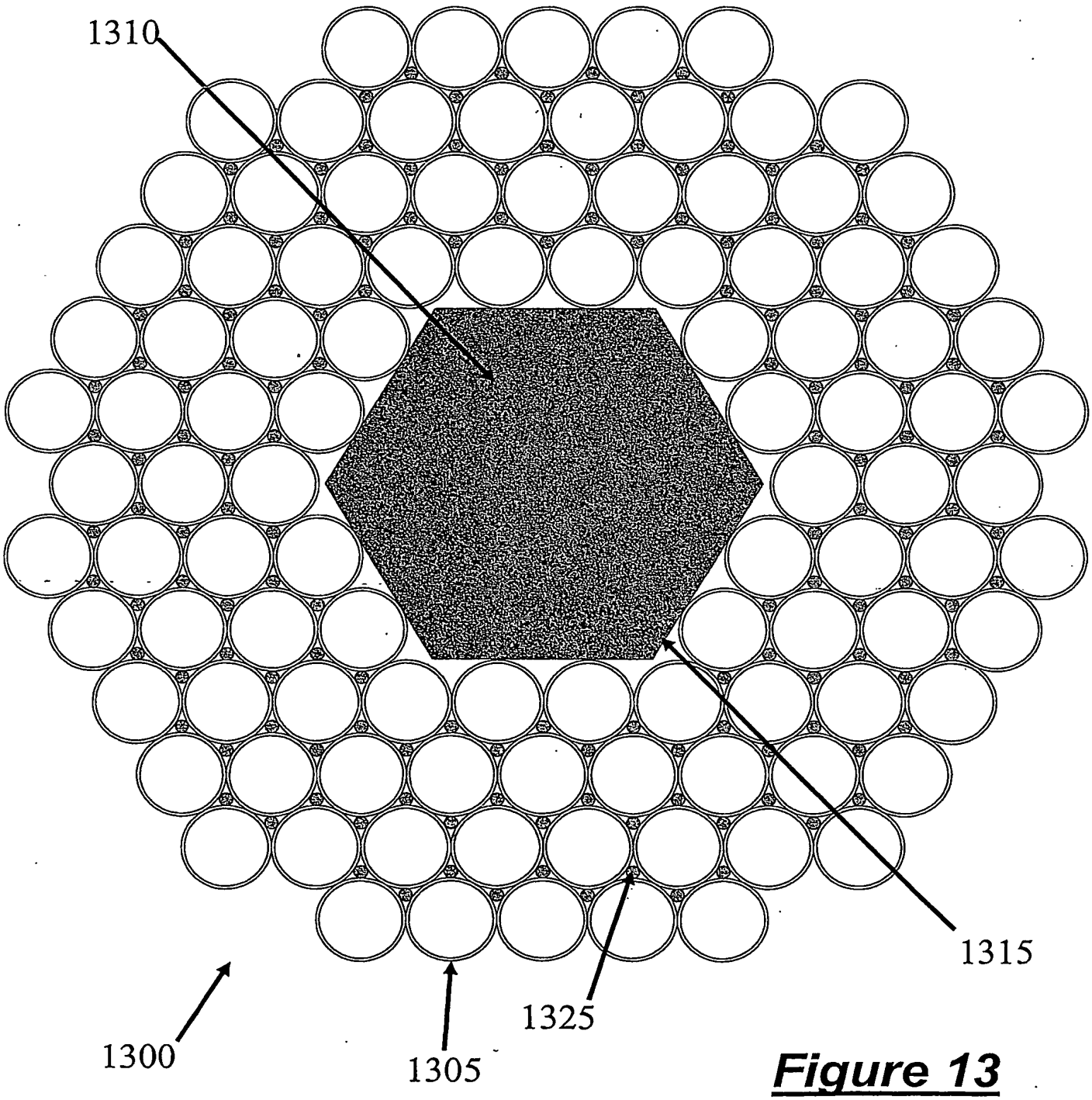

Figure 13

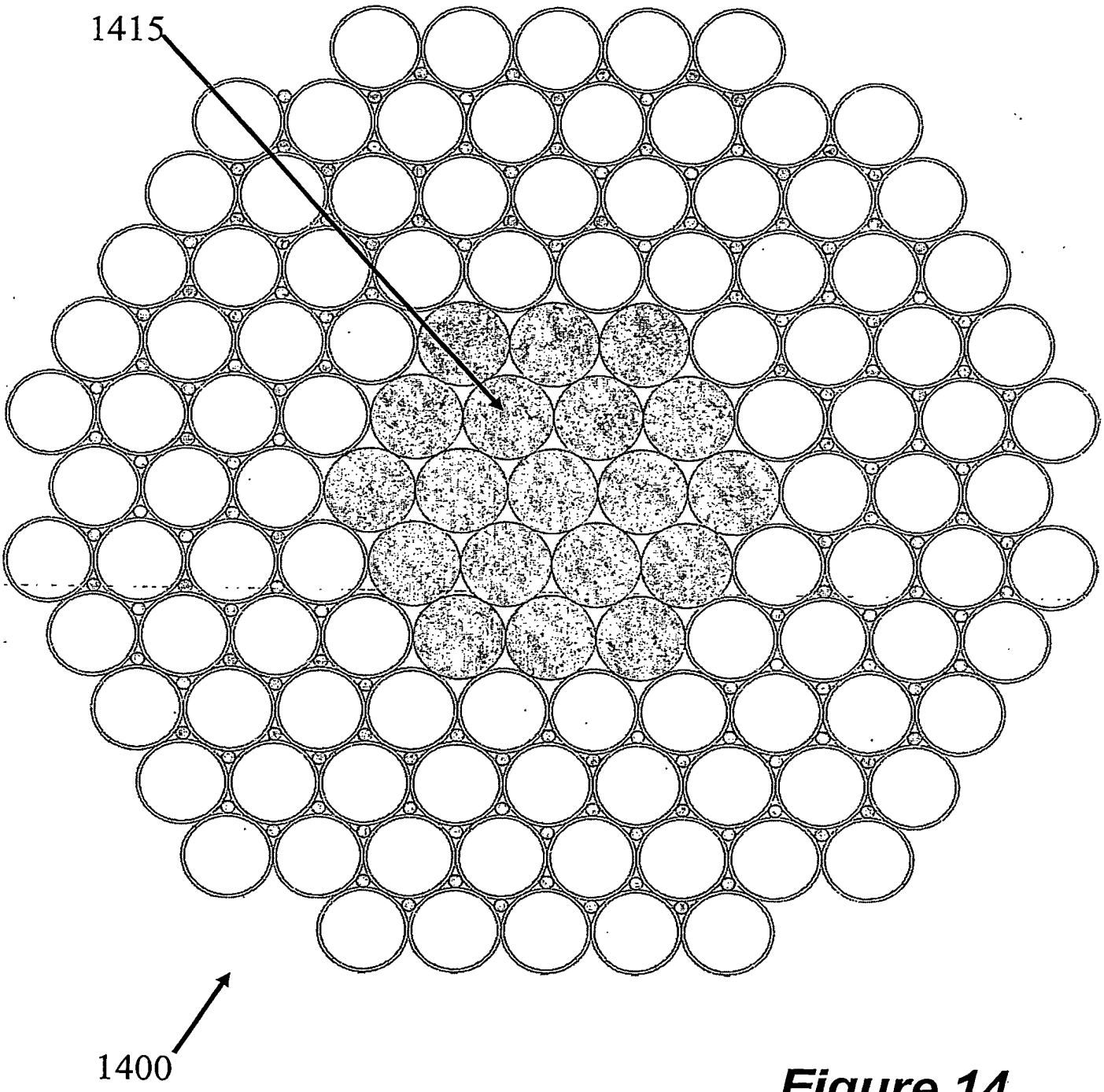

Figure 14

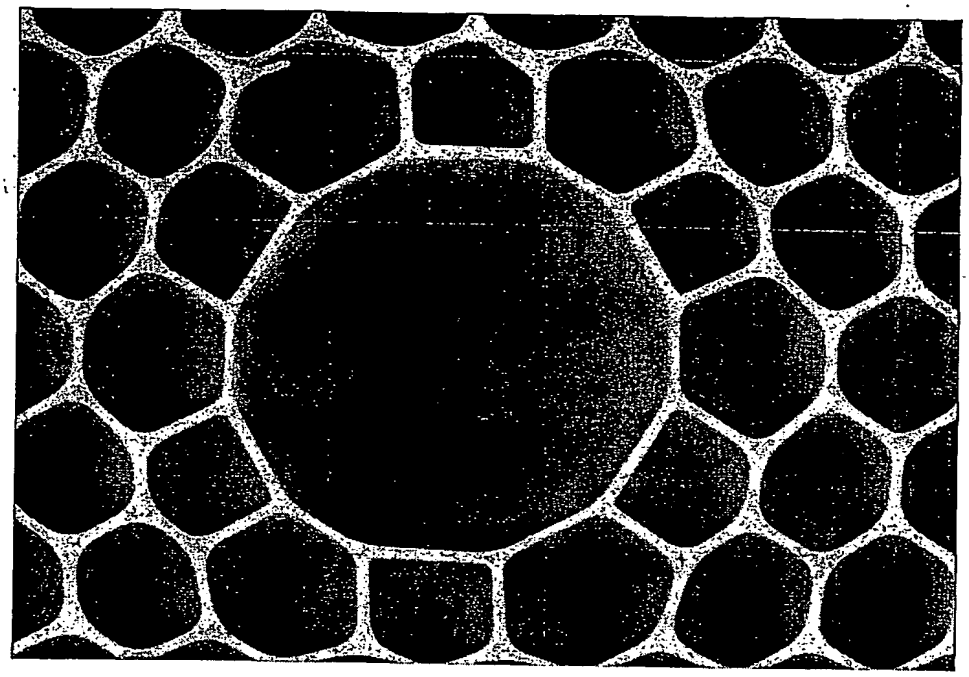

Figure 15a

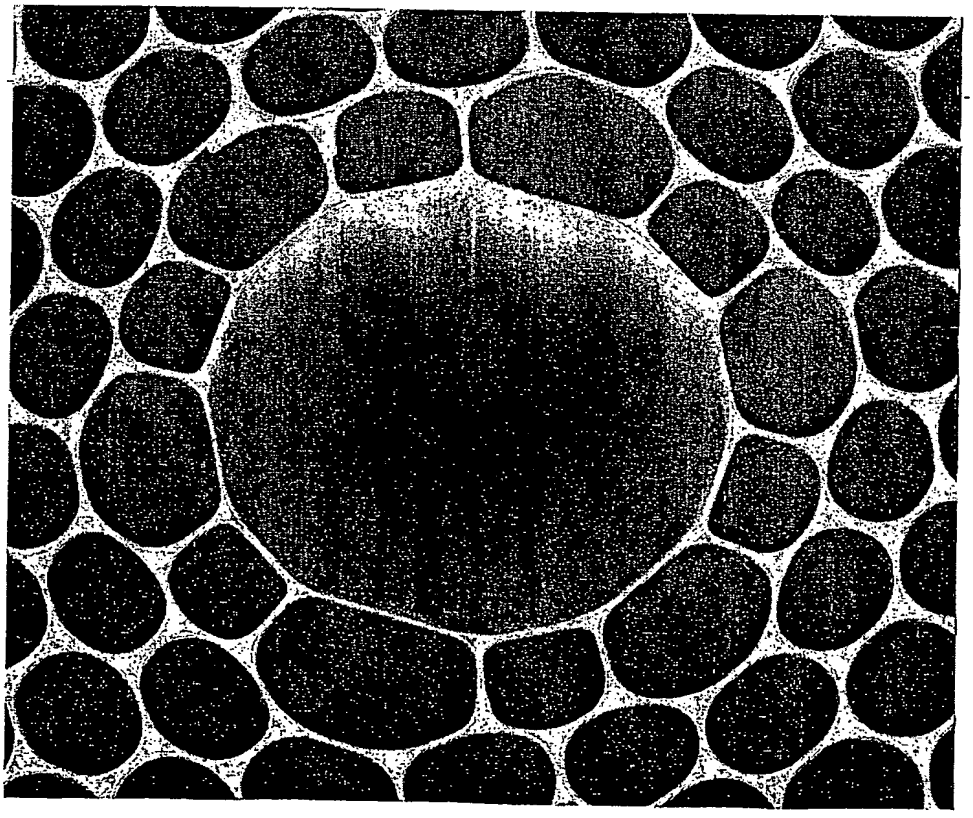

Figure 15b